CHAPTER

Snow avalanches

12

Jürg Schweizer, Perry Bartelt, and Alec van Herwijnen
WSL Institute for Snow and Avalanche Research SLF, Davos, Switzerland

Abstract

Snow avalanches are a major natural hazard in most snow-covered mountain areas of the world. They are rapid gravity-driven mass movements and are considered a meteorologically induced hazard. Snow avalanches are one of the few hazards that can be forecast, and in situ measurements of instability are feasible. Advanced hazard mitigation measures exist such as land-use planning based on avalanche dynamics modeling. The most dangerous snow avalanches start as a dry-snow slab avalanche that is best described with a fracture mechanical approach. How fast and how far an avalanche flows is the fundamental question in avalanche engineering. Models of different levels of physical complexity enable the prediction of avalanche motion. While the avalanche danger (probability of occurrence and expected size) for a given region can be forecast—in most countries with significant avalanche hazard, avalanche warnings are issued on a regular basis—the prediction of a single event in time and space is not (yet) possible.

12.1 Introduction

Snow avalanches occur in snow-covered mountain regions throughout the world and have caused natural disasters as long as mountainous areas have been inhabited or traveled. One of the oldest records dates back to 218 BC when Roman historian Livius described that Hannibal, while crossing the Alps, lost 12,000 soldiers and 2000 horses due to avalanches. Large disasters have often been associated with military operations such as the crossing of the Alps by Napoleon in 1800, the fighting in the Dolomites in 1916 during World War I, and most recently the conflict between India and Pakistan where, for example, an ice-rock-snow avalanche killed about 140 people in April 2012.

The number of avalanche fatalities per year due to snow avalanches is estimated to be about 250 worldwide. In fact, in Europe and North America alone, avalanches claimed the lives of about 1900 people during the 10-year period of 2000–01 to 2009–10. In addition to these well-established statistics, occasional large disasters occur in mountain countries in Asia. In Europe and North America, most of the fatalities nowadays involve personal recreation on public land, while avalanche fatalities on roads or in houses have become less frequent during the twentieth century due to extensive mitigation measures, including hazard mapping.

In Switzerland, for example, the number of avalanche fatalities on roads or in settlements was about 11 per year until the mid-1970s and has now decreased to less than three with a long-term total average

Snow and Ice-Related Hazards, Risks, and Disasters. https://doi.org/10.1016/B978-0-12-817129-5.00001-9

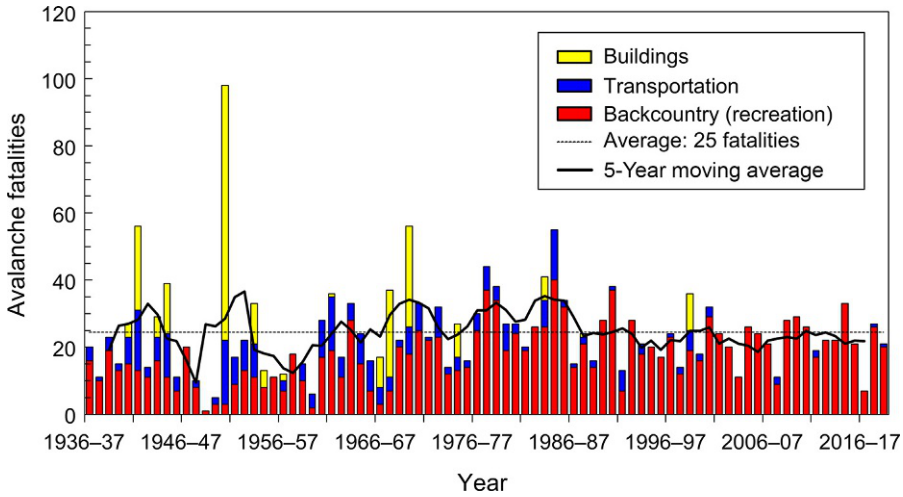

FIG. 12.1

Avalanche fatalities in the Swiss Alps for the period of 1936–37 to 2018–19 (83 years). Most victims were caught during recreational activities such as skiing ("Backcountry"); victims on roads including ski runs ("Transportation") and in villages ("Buildings") are far less frequent.

of 25 victims per year (Fig. 12.1). Since the disastrous avalanche winter in 1950–51 when 98 people in Switzerland (and 135 people in Austria) were killed (Fig. 12.2), Switzerland has constructed avalanche defense works worth about $1.5 billion. The effect of these mitigation measures was clearly shown during the winter of 1998–99 when a similar number of avalanches to that in the winter of 1950–51 released, but only 17 fatalities occurred (on roads or in buildings), despite the obvious increase in land use and mobility in the Swiss Alps (Fig. 12.3). The total damages amounted to $800 million (Wilhelm et al., 2001). In Canada, the yearly average direct and indirect costs are estimated to be more than $5 million (Jamieson et al., 2002).

Even if avalanches are a major threat to people living in and recreating near mountain communities, their contribution to the overall risk due to natural hazards in a country such as Switzerland is only about 3%—though they contribute more than one-third of all injuries and deaths. The risks due to an earthquake and flooding are estimated to be considerably higher in Switzerland primarily due to the larger area that is affected by these hazards so that damage to people, property, and infrastructure is expected to be higher than in the case of snow avalanches (BABS, 2003).

Avalanche risk analysis involves the determination of an avalanche return period or frequency and some measure of consequences that describe the destructive potential (CAA, 2016; McClung et al., 2002). To reduce avalanche risk, protective measures are often used in combination. Avalanche mitigation includes temporary measures (forecasting, road closure) and permanent measures (land-use planning, protective means such as snow sheds or tunnels, reforestation). By combining temporary and permanent measures in a cost-efficient way, otherwise known as integral risk management (Bründl and Margreth, 2021), the avalanche risk can be reduced to an acceptable level. Because snow avalanches are still relatively rare events, personal experience is limited and expertise is usually not readily available. Therefore, it is essential for hazard mitigation to increase the awareness of land managers, consultants, governmental agencies, and individual recreationists about snow avalanches.

FIG. 12.2

In Airolo (Switzerland), the Vallascia avalanche destroyed 23 buildings and killed 10 residents on February 12, 1951.

Photography: SLF archive.

FIG. 12.3

In Evolène (Switzerland), a large avalanche destroyed or damaged several chalets and killed 12 people on February 21, 1999.

Photography: M. Phillips.

Table 12.1 Avalanche size classification as widely used in Europe.

Size	Class label	Description	Typical volume (m^3)	Typical length (m)	Typical impact pressure (kPa)
1	Small	Unlikely to bury a person, except in runout zones with unfavorable terrain features (e.g., terrain traps)	100	30–50	1
2	Medium	Could bury, injure, or kill a person	1000	50–300	10
3	Large	Could bury a car, destroy a small building, or break a few trees	10,000	300–1000	100
4	Very large	Could destroy a railway car, large truck, several buildings, or a forest with an area up to 4 ha	100,000	1000–2000	500
5	Extremely large	Could destroy a village or forest of 40 ha	>100,000	>2000	1000

Based on McClung, D.M., Schaerer, P., 2006. The Avalanche Handbook. The Mountaineers Books, Seattle WA, U.S.A., 342 pp. and EAWS, 2020. Avalanche Size. https://www.avalanches.org/standards/avalanche-size/ (Accessed 12 May 2020).

12.2 The avalanche phenomenon

Snow avalanches are a type of fast-moving mass movement. They can additionally contain rocks, soil, vegetation, or ice. Avalanche size is classified according to its destructive power (EAWS, 2020; McClung and Schaerer, 2006; Table 12.1). For instance, a large slab avalanche may involve 10,000 m^3 of snow, equivalent to a mass of about 2000 t (snow density 200 kg/m^3). Avalanche speeds vary between 50 and 200 km/h for large dry-snow slides, whereas wet-snow avalanches are denser and slower (20-100 km/h). If the avalanche speed is high enough (>40–70 km/h), dry-snow avalanches generate a powder cloud.

Snow avalanches come in many different types (e.g., wet or dry) and sizes. The morphological classification published by the former International Commission on Snow and Ice (UNESCO, 1981) takes into account the three principal zones of an avalanche: origin (or starting zone), transition (or track), and runout (Table 12.2). It helps one to classify the type of avalanche based on observable features such as the manner of starting or the form of movement.

A snow avalanche path consists of a starting zone, a track, and a runout zone where the avalanche decelerates and the snow is deposited (Fig. 12.4). The starting zone, or in analogy to hydrology, the catchment area, is where the initial snow mass releases and usually consists of terrain steeper than 30 degrees. Occurrence of dry-snow avalanches originating from terrain under 30 degrees is very rare. Wet-snow slides, on the other hand, can occur on slopes under 25 degrees. Slope angle is the most important terrain factor influencing avalanche release. A snow avalanche will then flow downstream from the starting zone along the track, which often consists of creek beds and gullies. If the track is steep and a powder cloud develops, the powder snow avalanche may run straight down, regardless of the topography, that is, not follow, for example, any bends in the creek bed. While medium-sized avalanches may stop in the track (typically 15–30 degrees steep), very large ones can reach high velocities (up to 200 km/h) before reaching the runout zone

Table 12.2 International morphological avalanche classification (UNESCO, 1981).

Zone	Criterion	Characteristics	Denomination
Origin (starting zone)	Manner of starting	From a point	Loose-snow avalanche
		From a line	Slab avalanche
	Position of failure layer	Within the snowpack	Surface-layer avalanche
		On the ground	Full-depth avalanche
	Liquid water in snow	Absent	Dry-snow avalanche
		Present	Wet-snow avalanche
Transition (track)	Form of path	Open slope	Unconfined avalanche
		Gully or channel	Channeled avalanche
	Form of movement	Snow dust cloud	Powder snow avalanche
		Flow along ground	Flowing snow avalanche
Deposition	Surface roughness of deposit	Coarse	Coarse deposit
		Fine	Fine deposit
	Liquid water in snow	Absent	Dry avalanche deposit
		Present	Wet avalanche deposit
	Contamination of deposit	No apparent contamination	Clean avalanche
		Rock debris, soil, branches, trees	Contaminated avalanche

where they slow down and stop. On large avalanche paths the slope angle in the runout zone is usually less than 15 degrees (Jamieson, 2001). Runout zones for very large avalanche paths are generally on alluvial fans—a preferred area for infrastructure, including businesses and residences, in mountain areas.

12.3 Avalanche release

A snow avalanche may release in two distinctly different ways: as a loose-snow avalanche or as a snow slab avalanche (Fig. 12.5). Loose-snow avalanches start from a point, in a relatively cohesionless surface layer of either dry or wet snow. The initial failure originates in one location when a small mass of snow fails and begins to move and entrain additional snow. The process is analogous to the rotational slip of cohesionless sands or soil, but occurs within a small volume ($<1\,m^3$) in comparison with much larger initiation volumes in soil slides (Perla, 1980). As the snow mass descends, the avalanche spreads outward in an inverted V shape. Most loose-snow avalanches are relatively small and harmless because only a cohesionless surface layer is involved. However, when the entire snow cover is wet, loose-snow avalanches can entrain large volumes of snow and cause damage.

Snow-slab avalanches behave quite differently. They involve the release of a cohesive snow slab over an extended plane of weakness, analogous to the planar failure of rock slopes and landslides rather than to the rotational failure of soil slopes (Perla, 1980). The observed ratio between width and thickness of the slab varies between 10 and 10^3 and is typically about 10^2. Average slab thickness in the

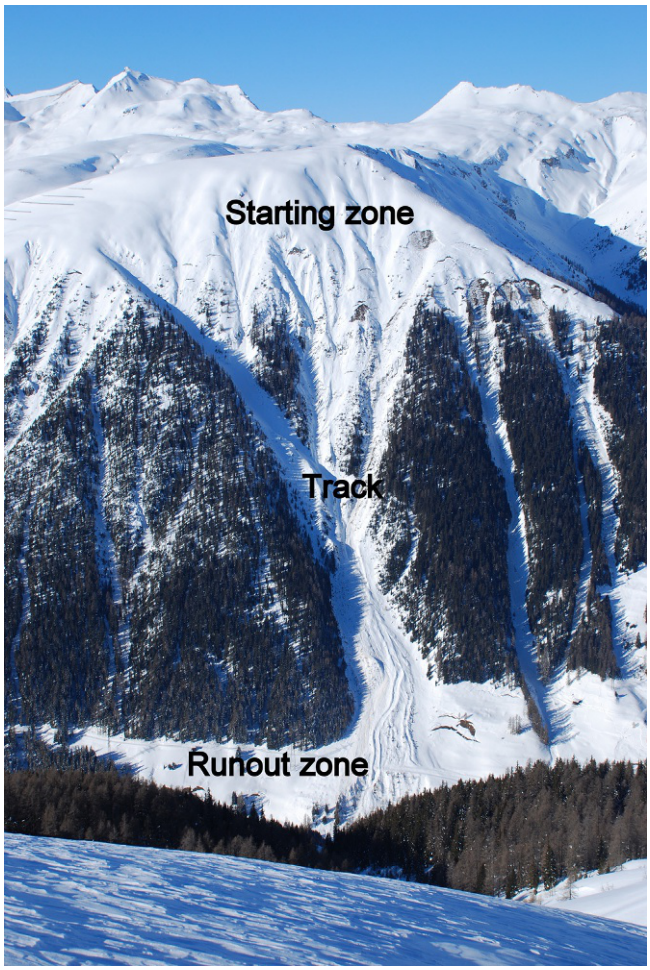

FIG. 12.4

Large avalanche path showing the starting zone where the avalanche initiates, the track, and the runout zone where the avalanche decelerates and the snow is deposited. Small avalanches may stop in the track, or even the starting zone.

Breitzug, Davos, Switzerland; photography: J. Schweizer.

starting zone is usually less than 1 m, typically about 0.5 m, but can reach several meters in the case of very large disastrous avalanches (Schweizer et al., 2003). Slab avalanches are the more hazardous of the two types and represent the vast majority of fatal avalanches. Slab avalanches are more harmful as they typically involve more snow and are harder to predict than loose-snow avalanches. Slab avalanches are the focus of most avalanche-related studies.

Predicting snow-slab avalanche release can be approached either: (1) by exploring the complex interaction between three main contributing factors: terrain, weather, and snowpack; or (2) by studying the physical and mechanical processes of avalanche formation (Schweizer et al., 2003). We will first

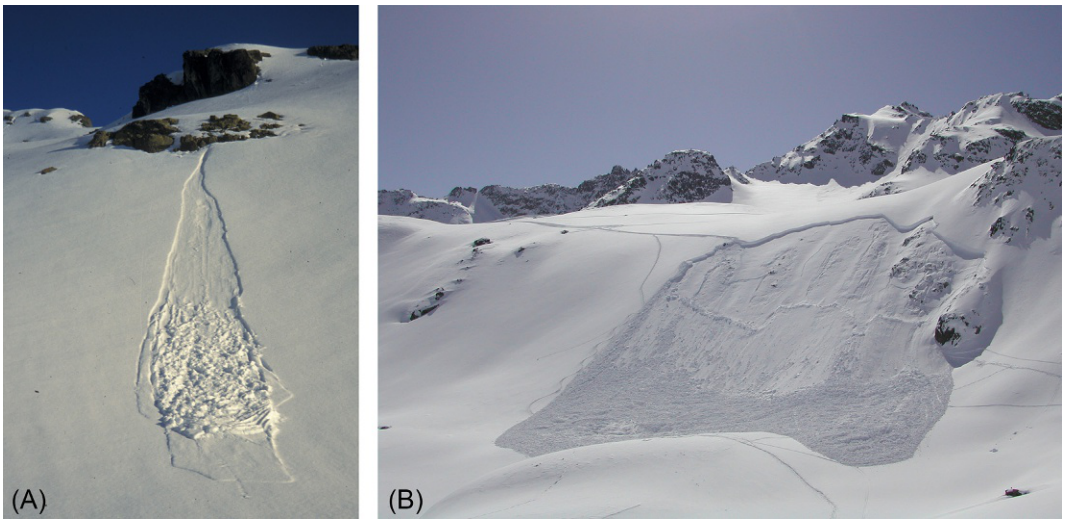

FIG. 12.5

Snow avalanches may release in two distinctly different ways: (A) as loose-snow avalanche or (B) as snow slab avalanche.

Photography: J. Schweizer.

discuss the former approach that is applied by most avalanche forecasting services. It involves empirically weighting the influence of the contributory factors in a specific situation.

Terrain is an essential factor and the only factor that is constant in time. A slope angle of about 30 degrees is required for a slab avalanches to release. However, other topographic parameters such as curvature, aspect, distance to a ridge, and forest cover are also important. In general, the identification of potential avalanche release areas is a difficult task requiring considerable expertise, but it is a prerequisite for large-scale hazard mapping, numerical avalanche simulations, and planning of hazard mitigation measures. Today, potential release areas (i.e., starting zones) can automatically be identified within a geographic information system (GIS), provided that a high-resolution digital terrain model (DTM) is available (Bühler et al., 2018). However, for detailed planning, including various release scenarios, manual adjustment of the release area perimeter is usually required. Forests inhibit avalanche formation; in particular, in dense forests the snow cover is too irregular to produce avalanches. The main effects that alter the snow cover characteristics in forests compared to open unfrosted terrain are: (1) the interception of falling snow by trees, (2) the reduction of near-surface wind speeds, (3) the modification of the radiation and temperature regimes, and (4) the direct support of the snowpack by stems, remnant stumps, and deadwood (Schneebeli and Bebi, 2004; Teich et al., 2012). Teich et al. (2019) showed that spatial variability in snow stratigraphy in forests is driven by percentage of canopy cover.

The main meteorological conditions contributing to avalanche formation are precipitation (new snow or rain), wind, air temperature, and solar radiation. For large, catastrophic avalanches, precipitation is the main driver. Although the total amount of precipitation plays an important role, the precipitation rate may also influence avalanche release. Wind contributes to loading and is often considered the most active contributing factor after precipitation. Loading by wind-transported snow can be fast and produce irregular deposits, increasing the probability of avalanching in certain areas.

Snow deposition by wind is strongly influenced by terrain so that snow-drift accumulations commonly occur at the same location year after year. The persistence of accumulation patterns has been revealed by terrestrial layer scanning (Prokop, 2008), suggesting that these patterns can be predicted based simply on topography and mean wind direction (Schirmer et al., 2011). Temperature and in general the energy balance at the snow-atmosphere interface can contribute to avalanche formation, especially in the absence of loading. Natural loose snow (point release) avalanches are often initiated by a rapid increase in solar radiation. For dry-snow slab avalanches, the effects of warming are complex and often subtle; a rapid increase in air temperature and/or solar radiation does not in general promote instability. In any case, instability always stems from changes in slab properties (Reuter and Schweizer, 2012; Schweizer and Jamieson, 2010a). Increased deformation due to reduced stiffness of the surface layers increases the strain rate in the weak layer, increases the energy release rate, or increases the skier stress at depth. While these effects occur rapidly and promote instability, delayed effects, such as snow metamorphism and settlement, tend to promote stability (McClung and Schweizer, 1999). Surface warming (of a dry snowpack) is most efficient with warming by solar radiation as radiation penetrates the surface layers where the energy is released. Surface warming due to warm (relative to the snow surface) air temperatures is a secondary effect—except in the case when a moderate or strong wind blows (Schweizer and Jamieson, 2010a).

Finally, snow cover stratigraphy is recognized as the key contributing factor for snow-slab avalanche formation (Schweizer et al., 2003). The mountain snowpack can contain many different snow layers with distinctive properties. Each layer is the result of a snowfall, wind transport, or energy exchange between the snow surface and the atmosphere. Each interface between two layers was once the snow surface and was influenced by the atmosphere before it was buried. Snow layers are generally characterized according to grain type, grain size, hardness, and density following the International Classification for Seasonal Snow on the Ground (Fierz et al., 2009). Some layers are softer so that the strain is concentrated within these layers (Reiweger and Schweizer, 2010); they have lower strength than the layers above and below, and are more often associated with slab avalanching and are hence termed weak layers. Some weak layers are very discernible within the snowpack and are several centimeters or even tens of centimeters thick. Other weak layers can be very thin (few mm) and hard to identify, but equally important. This weakness can be either within the old snow (typically a weak layer composed of facets, depth hoar, or surface hoar) or at the old snow surface underlying the new snow. Weak layers differ distinctly in grain size and hardness from the adjacent layers (Schweizer and Jamieson, 2003). They can be grouped into nonpersistent and persistent weak layers (Jamieson, 1995).

Nonpersistent weak layers, also called storm-snow instabilities, generally consist of precipitation particles that may remain weaker and lower in density than the adjacent layers during the initial stages of rounding (isothermal metamorphism; e.g., Kaempfer and Schneebeli, 2007). However, these layers tend to stabilize within a few days after burial, hence the name nonpersistent. In contrast, persistent weak layers can remain weak for extended periods of time, sometimes months. They consist of surface hoar, faceted crystals, or depth hoar; these layers have a strongly anisotropic microstructure (Walters and Adams, 2014) as their crystals generally were grown under strong temperature gradients. Due to their anisotropic microstructure, their mechanical behavior depends on the loading direction: They are more prone to failure in shear than in compression (Reiweger and Schweizer, 2013b). The observed failure behavior of these weak layers can be described with a closed-form failure envelope, accounting for failure both in shear and in compression (Chandel et al., 2014; Reiweger et al., 2015). This new mixed-mode shear-compression failure criterion was instrumental for prominent recent advances in

multiscale modeling of avalanche release (Gaume et al., 2017, 2018, 2019). The increased computer power and advanced snow characterization methods using X-ray computed tomography (Schneebeli and Sokratov, 2004) also allowed microstructure-based numerical models of snow behavior (Hagenmuller et al., 2014; Wautier et al., 2015), which reproduced the observed mixed-mode failure behavior of snow (Bobillier et al., 2020; Mede et al., 2018).

Although wet layers on the snow surface that freeze and become melt-freeze crusts form the bed surface for many slab avalanches, they are not considered weak layers. The failure often occurs in a layer of facets above the crust so thin it is hard to identify. These so-called weakly bonded crusts form when snow falls on a wet snow surface so that a weak layer of faceted crystals develops while the underlying wet layer freezes into a crust, often within a day (Conlan and Jamieson, 2016; Jamieson, 2006). With regard to avalanche accidents, persistent weak layers are the main concern for skiers as the majority of fatal avalanches occur on persistent weak layers (Schweizer and Jamieson, 2001).

Any loading by new or windblown snow or any temperature increase has no effect on snow stability if no weakness exists within the snowpack. The presence of a weak layer is a necessary, but not sufficient, condition for slab avalanche formation. Apart from the weak layer, the properties of the overlying slab are equally important for avalanche formation, in particular as deformational energy stored in the slab, which bends due to weak layer failure, is released and supports crack propagation.

The slab avalanche nomenclature (Perla, 1977) reflects the fact that a slab avalanche is the result of a fracture process involving at least four fracture surfaces. The first failure is within the weak layer, and the bed surface is defined as the surface over which the slab slides. The bed surface can be the ground or older snow. The weak layer is always just above the bed surface and just under the slab. The breakaway wall at the top periphery of the slab is called the crown (fracture) and is approximately perpendicular to the bed surface reflecting the fact that the initial failure is in the weak layer below the slab. The flanks are the left and right sides of the slab. The flanks are usually smooth surfaces, as is the crown. The lowest downslope fracture surface is termed the stauchwall (Fig. 12.6) (Schweizer et al., 2003).

Depending on the processes leading to slab release, three types of slab avalanches occur: dry-snow, wet-snow, and glide-snow avalanches.

12.3.1 Dry-snow avalanches

The release of a dry-snow slab avalanche is due to overloading an existing weakness in the snowpack. Most dry-snow slab avalanches start naturally during or soon after snow storms (Heck et al., 2019a). High precipitation rates favor snowpack instability. In general, about 50 cm of new snow within 24 h (equivalent to about 50 mm of precipitation) is critical for avalanche initiation. Large disastrous avalanches usually follow storms that deposit more than 1 m of snow. Therefore, for large new snow avalanches, the 3-day sum of precipitation is the strongest forecasting parameter (Schweizer et al., 2009) and closely related to avalanche danger (Schweizer et al., 2003). The triggering of a dry-snow slab avalanche can also occur artificially by localized, rapid, near-surface loading by, for example, people (usually unintentionally) or intentionally by an explosion (igniting a gas mixture or solid explosives) as part of avalanche control programs (Simioni et al., 2015, 2017). In general, naturally released avalanches mainly threaten residents and infrastructure, whereas human-triggered avalanches are the main threat to recreationists (Schweizer et al., 2003).

For a dry-snow slab avalanche to release (Schweizer et al., 2016a), an initial crack in a weak layer has to propagate below the slab. For natural slab avalanches, it is believed that the initial failure is

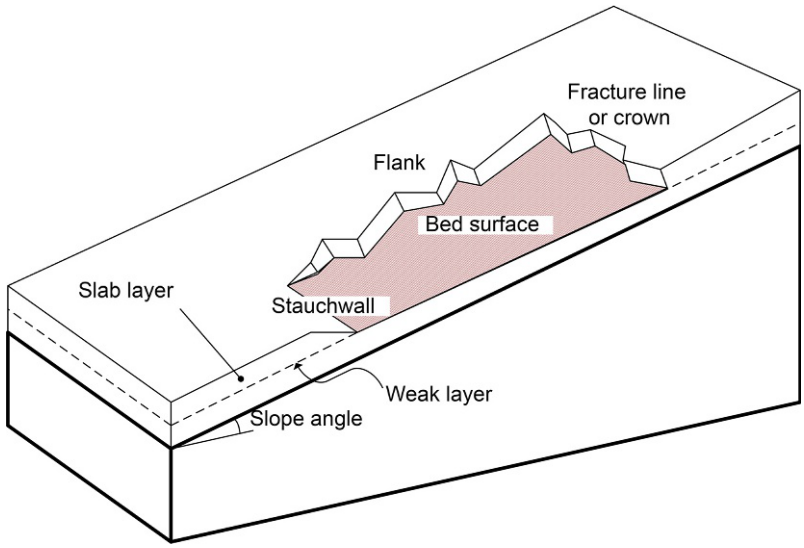

FIG. 12.6

Slab avalanche nomenclature.

Based on Schweizer, J., Jamieson, J.B., Schneebeli, M., 2003. Snow avalanche formation. Rev. Geophys. 41(4), 1016.

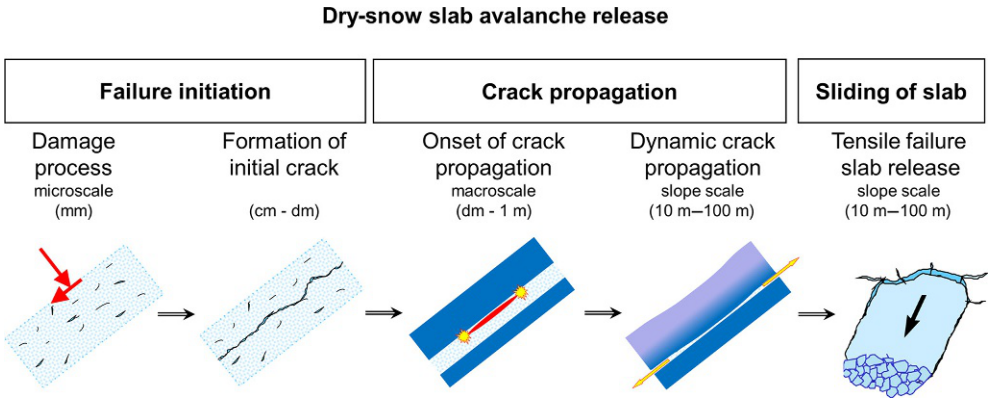

FIG. 12.7

Conceptual model of dry-snow slab avalanche release.

Modified from Schweizer, J., Reuter, B., van Herwijnen, A., Gaume, J., 2016a. Avalanche release 101. In: Greene, (Ed.), Proceedings ISSW 2016. International Snow Science Workshop, Breckenridge CO, U.S.A., 3–7 October 2016, pp. 1–11.

caused by a gradual damage process at the microscale leading to failure localization within the weak layer (Fig. 12.7) manifested by acoustic emissions (Capelli et al., 2018). For artificially triggered avalanches (e.g., skier-triggered avalanches) the external trigger induces localized deformations that are large enough to initiate a crack within the weak layer (van Herwijnen and Jamieson, 2005). In either case, if the initial crack in the weak layer reaches a critical size (length)—of the order of several tens of

centimeters—it will propagate through the weak layer below the slab. After failure, the very porous character of the weak layer leads to its volumetric collapse (van Herwijnen et al., 2010) and thus closing of crack faces due to the weight of the overlaying slab, which is also referred to as anticrack (Heierli et al., 2008). This complex process of weak layer collapse explains why avalanches that release on steep slopes can be triggered from flat terrain (called remote triggering). Hence on low-angle terrain, weak layer collapse, which should not be mistaken for a failure mode, is essential to describe crack propagation, whereas on steep slopes collapse is negligible and shear is the dominant driver of crack propagation (Gaume et al., 2019). Once the weak layer has fractured, slab and bed surface come into contact. If the gravitational pull on the detached snow slab is large enough to overcome friction—that is, the slope is steep enough (>30 degree)—a snow slab avalanche is released (van Herwijnen and Heierli, 2009). This fracture mechanical view spans several orders of magnitude from the scale of bonds in the weak layer to the scale of an avalanche on a snow slope. Only recently, the first model was presented that successfully spans these scales. Using the material point method, Gaume et al. (2018) simulated both the release (failure initiation and dynamic anticrack propagation in the weak layer) and the flow of the avalanche.

Describing avalanche release as a fracture mechanical process dates back to McClung (1979, 1981a) who adapted a failure model by Palmer and Rice (1973). Two decades later, Kirchner et al. (2000) performed the first fracture mechanical measurements needed to eventually apply models based on fracture mechanics. Following laboratory measurements (Schweizer et al., 2004) a field test was developed, the propagation saw test (PST; Gauthier and Jamieson, 2006; Sigrist and Schweizer, 2007; van Herwijnen and Jamieson, 2005) that now, using particle tracking velocimetry (PTV), enables the determination of two crucial properties: the specific fracture energy of the weak layer and the stiffness of the slab (Schweizer et al., 2011; van Herwijnen et al., 2016).

12.3.2 Wet-snow avalanches

Wet-snow avalanches release due to weakening as liquid water percolates into the snow cover; they primarily endanger communication lines and infrastructure. Wet-snow avalanches mostly release spontaneously and often cannot be triggered artificially—in contrast to dry-snow avalanches. Although dry-snow avalanches cause most avalanche fatalities, mainly among winter recreationists, wet-snow avalanches may occasionally cause severe damage. Analysis of a 10-year record of avalanche victims in the Swiss Alps showed that about 50% of the fatalities caused by naturally released snow avalanches were due to wet-snow avalanches (either slab or loose-snow avalanche) (Schweizer and Lütschg, 2001). When only considering human-triggered avalanches, however, fatalities due to wet-snow avalanches drop to 1%. Hence, spontaneous releases of wet-snow avalanches are as lethal as naturally released dry-slab avalanches, but wet-snow avalanches are seldom triggered by recreationists themselves. Our understanding of the triggering conditions for wet-snow avalanches is still somewhat limited. This is partly due to a lack of observations, and the fact that wet-snow instability is a highly transient and spatially variable phenomenon related to the water transport in snow (Schneebeli, 2004).

Two prerequisites for wet-snow avalanche formation exist: (1) Liquid water must be present within the snowpack; and (2) a (large) part of the snowpack must be isothermal (0°C). Liquid-water content in the seasonal snowpack rarely exceeds a few percent per volume (Heilig et al., 2015). Water production at the snow surface is determined by the energy balance at the snow-air interface and/or the amount of water delivered through rain (Mitterer and Schweizer, 2013). Based on experience and observations, three possible triggering mechanisms were suggested (Baggi and Schweizer, 2009): (1) loss of strength

due to water infiltration and storage at a capillary barrier, (2) overloading of a partially wet and weak snowpack due to precipitation, and (3) gradual weakening of the snowpack due to warming to 0°C and eventual failure of basal layers. Clearly, combinations of these three mechanisms may exist. Overall, it is still not entirely clear how water infiltration influences wet-snow instability. Snow stratigraphy is key as it controls the rate of infiltration, the pattern of infiltration, and the concentration of water at a given location—which then ultimately will affect the mechanical strength (Peitzsch, 2008). Yamanoi and Endo (2002) observed a continuous decrease in shear strength with increasing liquid-water content (up to 8%). Recent preliminary results of shear measurements on different substrates indicate that the decrease is highly nonlinear.

Wet-snow avalanches are particularly difficult to forecast. Once the snowpack becomes partly wet, the release probability rapidly increases, but determining the peak and end of a period of high wet-snow avalanche activity is particularly difficult (Techel and Pielmeier, 2009).

Air temperature is commonly related to days with wet-snow instability (Kattelmann, 1985), but is not suitable for forecasting wet-snow avalanches since many false alarms are produced (Mitterer and Schweizer, 2013; Trautman, 2008). Combining air temperature with either incoming solar radiation or snow surface temperature generally improves the predictive performance for days with high wet-snow avalanche activity improved (Helbig et al., 2015; Mitterer and Schweizer, 2013). In addition, Mitterer and Schweizer (2013) showed that when modeling the entire energy balance for virtual slopes, avalanche and nonavalanche days could be classified with good accuracy. However, modeling and interpreting the energy balance in terms of wet-snow avalanche release probability is complex and sometimes not feasible for operational avalanche forecasting. Therefore, Mitterer and Schweizer (2013) introduced a liquid-water content index describing the amount of liquid water in the entire snowpack calculated with the numerical snow cover model SNOWPACK (e.g., Lehning et al., 1999). The index related well to observed wet-snow avalanche activity and indicated spatial and temporal patterns of wet-snow avalanche activity. Onset and peak of wet-snow avalanche activity were mostly well detected, particularly when high temperatures and high values of shortwave radiation caused the percolating meltwater. However, determining the end of a period with wet-snow avalanche activity was not possible, because the index showed no distinctive pattern at the end of such periods. The approach can also be applied in forecast mode by driving SNOWPACK with output from a numerical weather-prediction model (Bellaire et al., 2017). Alternatively, Wever et al. (2016) investigated whether ponding of water at capillary barriers was indicative of wet-snow avalanche occurrence. They found a liquid-water content of 5%–6% locally within the snow cover to be a good predictor for wet-snow avalanche activity. In addition, the location or depth within the snow cover where the liquid-water content was highest was found to be related to the size of wet-snow avalanches.

12.3.3 Glide-snow avalanches

Glide-snow avalanches can represent a serious challenge to avalanche programs protecting roads, towns, ski lifts, and other infrastructure. These avalanches are notoriously difficult to forecast and can be very destructive, as large volumes of dense snow are mobilized at once (Höller, 2014; Mitterer and Schweizer, 2012). Glide-snow avalanches occur when the entire snowpack glides over the ground until an avalanche is released. Glide cracks, that is, full-depth tensile cracks exposing the ground, are often observed before glide-snow avalanching (Fig. 12.8). Glide-snow avalanches mostly release from specific and well-known starting zones (Lackinger, 1987; Leitinger et al., 2008). They occur mostly on steep terrain, that is, 30–40 degree steep slopes (Leitinger et al., 2008; Newesely et al., 2000), covered with smooth rock

FIG. 12.8

Glide-snow avalanches are often preceded by the appearance of a glide crack through the snow cover. Avalanche release can occur within minutes, hours, or weeks, or not at all.

Photography: R. Meister.

(e.g., Stimberis and Rubin, 2011), grass (in der Gand and Zupančič, 1966), or tipped-over bamboo bushes (Endo, 1985). Newesely et al. (2000) observed increased snow gliding on abandoned pastures compared to slopes with short grass. Leitinger et al. (2008) and Höller (2001) noted that the lack of dense forest stands contributed to glide-snow activity, in particular if the distance between surrounding anchor points is larger than 20 m. Observations suggest that most glide-snow avalanches release on convex rolls (e.g., in der Gand and Zupančič, 1966).

Snow gliding processes and glide-snow avalanches are conceptually well understood, and it is widely accepted that a reduction in friction at the base of the snow cover due to the presence of liquid water is the main driver (e.g., Lackinger, 1987; McClung, 1981b). Once friction is reduced and a glide crack has opened, the peripheral strength, in particular of the stauchwall, seems to be crucial for stability (Bartelt et al., 2012a). Because various processes are involved in reducing friction at the base of the snow cover, the relationship between meteorological conditions and glide-snow avalanching is complex. Thus, relying on weather data to forecast glide-snow avalanches is still difficult and relatively inaccurate (Peitzsch et al., 2012; Simenhois and Birkeland, 2010; Stimberis and Rubin, 2005). As the presence of water seems decisive for the formation of glide-snow avalanches, it is paramount to know the processes that are responsible for the presence of water at the snow-soil interface. Three different processes may deliver liquid water to the snow-soil interface (McClung and Clarke, 1987): (1) water percolating through the snow cover, (2) heat released from the warm ground melting the snow at the base of the snow cover after the first major snowfall, and (3) water, produced at terrain features with strong energy release (e.g., bare rocks), running downward along the snow-soil interface or originating from springs (groundwater outflow). In addition, Mitterer and Schweizer (2012) suggested that the

lowermost snowpack layer becomes wet due to capillary rise caused by different hydraulic pressures along the snow-soil interface. In fact, Ceaglio et al. (2017) recently observed increased glide rates for high values of liquid-water content in the underlying soil.

The triggering case (1) is very similar to the triggering process related to wet-snow avalanches: The less permeable substrate below the snowpack often acts as a capillary barrier to infiltrating water. Thus, determining the arrival time of water at the base of the snow cover is crucial for predicting glide-snow avalanches (Mitterer et al., 2011). The main processes associated with producing the water are due to melting at the snow surface and rain-on-snow events. Many glide-snow avalanches are therefore observed during warm periods or rain events (Clarke and McClung, 1999; Lackinger, 1987). However, there are also so-called cold temperature events that release when the snow cover is still mostly below freezing. in der Gand and Zupančič (1966) stated that for these events the existence of a lowermost moist snow layer is especially important as a dry boundary layer would not cause glide motion on a grass surface. Moreover, they suggested that liquid water is produced due to warm ground temperatures. Snow layers with low temperatures (below 0°C) may exist above the wet layer. These observations have been confirmed by several later studies (Höller, 2001; Newesely et al., 2000). In addition, the release of glide-snow avalanches, in particular cold snow events, is often observed during snow loading as the additional load increases creep and glide (Dreier et al., 2016).

The reduction of friction at the base of the snow cover results in increased snow glide rates, and glide rates are closely related to glide-snow avalanche release (e.g., in der Gand and Zupančič, 1966). Clarke and McClung (1999) and Stimberis and Rubin (2011) suggested that glide-snow avalanche release may best correlate with periods of rapid increases in glide rates. Thus, measuring glide rates could improve glide-snow avalanche forecasting. Several methods have been used to measure glide rates in snow, including sprung probes (Wilson et al., 1997), seismic sensors (Lackinger, 1987; Stimberis and Rubin, 2005), accelerometers (Rice et al., 1997), and most frequently, glide shoes (Clarke and McClung, 1999; in der Gand and Zupančič, 1966; Lackinger, 1987; Stimberis and Rubin, 2005). Although all these methods can be used to measure glide rates, they are currently costly, somewhat unreliable, and difficult to conduct in multiple paths.

More recently, a different approach for measuring glide rates was proposed by tracking the expansion of glide cracks with time-lapse photography (van Herwijnen et al., 2013; van Herwijnen and Simenhois, 2012) (Fig. 12.9). When a glide crack appears, the ground below the snow cover is exposed. Since the ground is much darker than snow, it can clearly be identified on the time-lapse images. Using a simple method based on dark pixel counting, glide rates can be derived. van Herwijnen and Simenhois (2012) showed that for glide cracks that resulted in avalanche release, the number of dark pixels rapidly increased a few hours before avalanche release, in line with previously published glide rate measurements. Although such new developments are encouraging with regard to glide-snow avalanche forecasting, it is still not clear how increases in glide rates relate to avalanche release. Alternatively, radar interferometry can be employed to monitor snow displacements on slopes (Caduff et al., 2015)—independent of visibility, which is required for time-lapse photography.

12.4 Avalanche flow

Avalanche flow begins after snow is released and set in motion. How fast and how far an avalanche flows are two of the essential questions in avalanche engineering. Hazard maps and the planning of mitigation measures require an estimation of avalanche speed and the extent of the inundated area

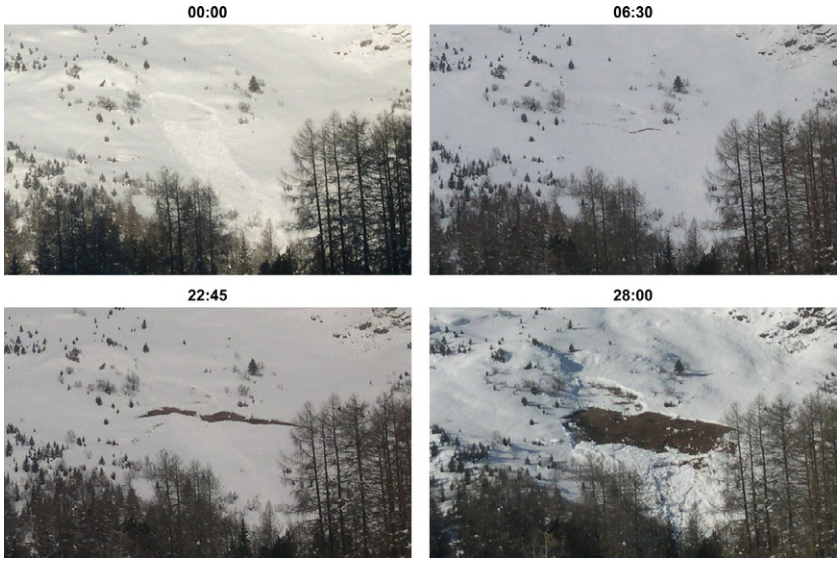

FIG. 12.9

Sequence of images showing the gradual expansion of a glide crack, followed by the release of a glide-snow avalanche after 28 h.

Photography: A. van Herwijnen.

as a function of the release zone location and characteristics of the mountain terrain (steepness, roughness, gullies, vegetation, etc.). Hazard scenarios are typically based on the concept of avalanche-return period, which is linked to snow-cover fracture heights (e.g., Ancey et al., 2004; Bründl et al., 2010). Information regarding snowfall history and past avalanche events is necessary in order to predict reasonable starting masses, which greatly affect avalanche runout distances. Climatic conditions need to be considered to assess the possibility of extreme wet-snow avalanches or powder snow avalanches. To predict the motion of avalanches including these effects, models with different levels of physical complexity are employed in engineering practice. These include empirical (e.g., Lied and Bakkehoi, 1980), statistical (e.g., McClung and Mears, 1991), and physical and semiphysical analytical models (e.g., Salm et al., 1990). Increasingly physics-based numerical models (e.g., Christen et al., 2010; Sampl and Zwinger, 2004) are being used. The newest generation numerical models run on high-resolution digital elevation models (Bühler et al., 2013) and also account for snow entrainment processes, which allow the treatment of increasing mass during avalanche motion.

12.4.1 The transition to flow: Slab breakup and snow granularization

When a dry-snow slab avalanche releases, it may first slide as a rigid block. For dry-snow avalanches, the sliding surface is typically a harder (older) snow layer; for wet-snow avalanches, the sliding surface can be the ground. Friction is low because the slab often slides on a hard layer lubricated by the poorly bonded remnants of the fractured weak layer; wet-snow avalanches commonly slide on wetted surfaces. Because of the low friction of the sliding surface, sliding snow can reach velocities of over 10 m/s. Terrain undulations or variations in surface roughness contribute to the quick breakup of

FIG. 12.10

The breakup of the slab and the start of a large flowing avalanche.

Photography: T. Feistl.

the slab (Fig. 12.10). First, large snow cover fragments form, but as the slab continues to displace, the fragments disintegrate into smaller granules of various shapes and sizes (Bozhinskiy and Losyev, 1998). By the time the entire slab has exited the release zone and passed the stauchwall (which can also enhance the breakup process), the slab avalanche has transformed into a granular flow.

The bulk flow density of the avalanche is given by the distribution of granules within an avalanche flow volume. The breakup process, granule collisions, and other interparticle interactions lead to hardened granules and snow fragments. Typical granule densities range between 300 kg/m^3 and 500 kg/m^3 (Bozhinskiy and Losyev, 1998). It is also possible to find hard ice granules in avalanche deposits as well as rocks and woody debris (Fig. 12.11).

The bulk flow densities of the avalanche can vary strongly (Gauer et al., 2007, 2008). For example, highly fluidized avalanches—a dry-snow flowing avalanche or powder snow avalanche—can have bulk flow densities at the front of less than 100 kg/m^3. Such regions in the avalanche are often termed "saltation" layers because of their low solid mass content (Gauer et al., 2008). Wet-snow avalanches or the dense core of flowing avalanches have higher bulk-flow densities, varying between 200 and 400 kg/m^3, that is, with bulk densities near the granule densities, suggesting less interstitial air space. Avalanches, depending on the snow properties and the granule formation, can exhibit both "collisional" and "frictional" flow regimes. It is entirely possible that with one single avalanche a transition between flow regimes will occur (Bartelt et al., 2011; Köhler et al., 2018). For example, at the head of a dry-snow flowing avalanche or powder avalanche we often are confronted with a collisional regime or dispersed, dilute-flow regime, whereas toward the tail of the avalanche the flow densifies, producing the dense core of the avalanche. An understanding of the avalanche flow density is necessary as it determines both the mobility of the flow and the magnitude of the avalanche impact pressures.

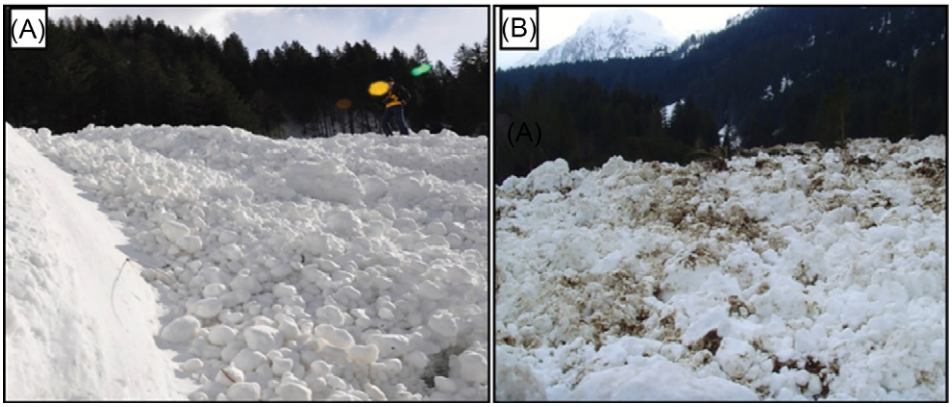

FIG. 12.11

The granular deposits of (A) dry-snow flowing avalanche and (B) wet-snow avalanche.

Photography: P. Bartelt.

The second salient feature of the granularization process is that it modifies the internal energy fluxes of the avalanche (Fig. 12.12) (Bartelt et al., 2006). When a slab releases, potential energy P is transformed into kinetic energy K and heat E. This kinetic energy is associated with the mean slope-parallel movement of the avalanche, the velocity U. Frictional processes dissipate the kinetic energy, raising the internal heat energy E of the avalanche. In this model of avalanche flow (Fig. 12.12), the motion of the avalanche can be described completely, once the frictional processes have been defined. This flow model is the basis of many (useful) block-type avalanche models (Perla et al., 1980; Salm et al., 1990). However, the granularization of the snow slab at release changes this simple energy model dramatically. As the slab displaces, space opens up between the granules. Movements in the slope-perpendicular direction are possible, implying an increase in the avalanche flow volume and a decrease in the avalanche flow density. This energy, denoted R_v, is termed "configurational" as it is associated with volume changes and therefore with flow densities and flow regimes. Importantly, the granules no longer all move with the same speed or direction of the mean flow. That is, the avalanche motion is no longer a rigid block, but a highly variable and deformable mass of particles. This energy has been termed R_k for "random kinetic" as it is associated with granule movements that vary from the mean translational velocity (Bartelt et al., 2006; Buser and Bartelt, 2009).

12.4.2 Avalanche flow regimes

After the transition phase of release and slab breakup, the flow phase begins. The avalanche at first accelerates and reaches a maximum velocity (transition zone) before decelerating on a flatter slope (runout zone). The length of the transition and runout phases depends on the geometry of the avalanche path, but also on the avalanche type and the frictional properties of the flowing snow (Fig. 12.13).

Mitigation of snow-avalanche hazard requires determining the propagation speed of the leading edge, the avalanche-flow density, and the dimensions of the avalanche body (depth, width, length).

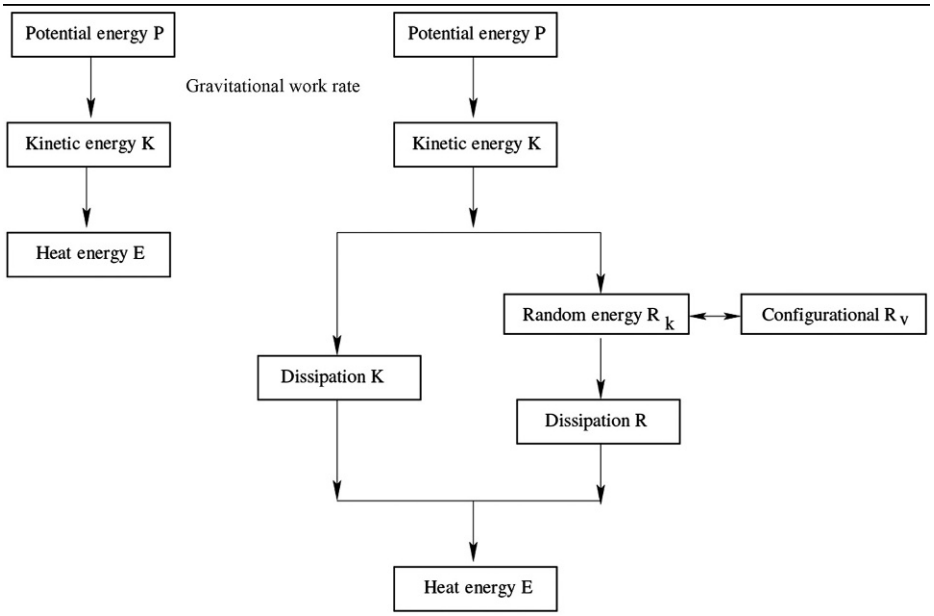

FIG. 12.12

Energetics of avalanche flow. (Left) In most block and simple hydrodynamic models, potential energy is transformed into kinetic energy and then by frictional processes to heat. (Right) In granular flow models, potential energy is similarly transformed into kinetic energy. However, shearing in the avalanche core creates both microscopic random energy (heat) and macroscopic random energy (granular temperature, R_k). Some of the shearing energy changes the density of the avalanche flow (configurational energy R_v). All potential is dissipated to heat when the avalanche comes to rest.

FIG. 12.13

The muddy deposits of a large wet-snow avalanche near Klosters (Switzerland), April 2008.

Photography: P. Bartelt.

These parameters vary over the length of the avalanche track, from the point of release to the point of maximum runout. The total volume of avalanche deposits is often an additional parameter that is required to dimension the height of avalanche dams and avalanche deflecting structures.

The problem of predicting avalanche flow in mountain terrain is difficult. Many different models have been developed to estimate avalanche-flow parameters. The models are based on relatively simple observations of avalanche drop height vs. runout, or on detailed flow measurements (Harbitz, 1998). The models, for example, can be simple, empirical formulas that average terrain features, or more intricate numerical models that require digital elevation models to represent the complexities of real mountain terrain. To date, however, both simple and complex models divide avalanche flow into one of two flow distinct and general categories: *dense flowing* and *powder* (suspension). This division essentially splits avalanche flow into a regime (or model) with relatively dense snow mass ($\rho = 100$–$500\,\mathrm{kg/m^3}$) and a regime (or model) of highly dispersed snow and air mass ($\rho = 3$–$50\,\mathrm{kg/m^3}$). The dispersed phase can be further subdivided into a "saltation layer" ($\rho = 10$–$50\,\mathrm{kg/m^3}$) and a "suspension layer" ($\rho = 3$-$10\,\mathrm{kg/m^3}$). Dry-mixed avalanches consist of a combination of both dense and powder parts and therefore consist of a dense core with saltation and suspension layers (Fig. 12.14). See Gauer et al. (2008) for an overview of inferred density measurements in snow avalanches.

Here it is important to reiterate that avalanches are composed of flowing snow debris mixed with air, and the very fact that avalanche density varies is a result of the granularization and breakup process

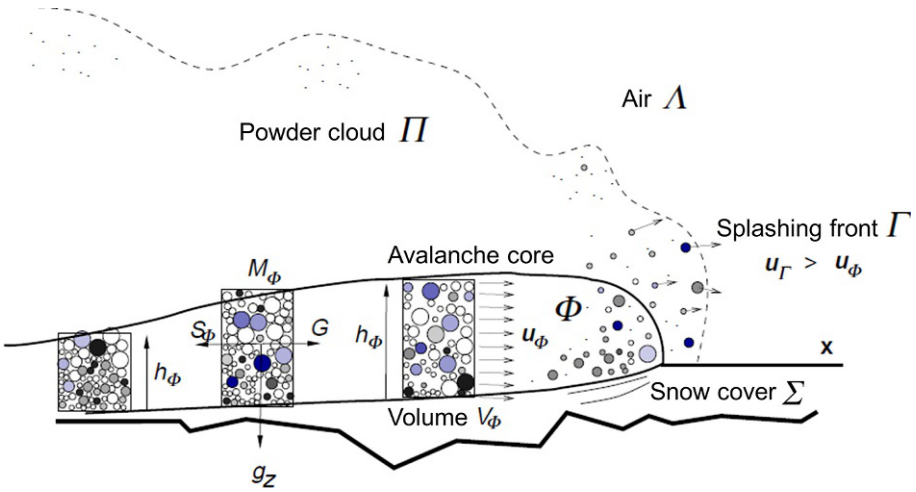

FIG. 12.14

Avalanche cross section. Mixed flowing/powder snow avalanches consist of a dense avalanche core Φ and a suspension layer Π. The core of height h_Φ consists of compacted snow granules. The speed of the avalanche core u_Φ is defined by the balance between the driving force of gravity G (terrain slope) and avalanche friction S_Φ (surface roughness, flow density). The avalanche can entrain the snow cover Σ increasing the size (mass M_Φ and volume V_Φ) of the avalanche. The density of the core (the number of particles in the volume V_Φ) can change from the avalanche front to tail. The cloud Π contains suspendable ice dust. The cloud entrains the surrounding air Λ, diluting the density of the cloud, and producing immense cloud heights. At the front of the avalanche, particles are ejected, often at speeds u_Γ higher than the core velocity $u_\Gamma > u_\Phi$, producing a saltating prefront of snow particles.

that allows density variations. Therefore, flow regime and flow regime transitions are intricately related to the granular properties of flowing snow, which are strongly temperature and moisture dependent (Gauer et al., 2008; Steinkogler et al., 2015).

12.4.3 The avalanche core

The dense and saltation layers can be grouped together to form the *avalanche core*. This is the destructive center of the avalanche. The core contains mass in granular form, that is, both large and small aggregates of ice grains. Mean granule sizes for dry-snow avalanches are in the range of 5–10 cm; wet-snow granules are larger, a result of the cohesive properties of moist snow (Bartelt and McArdell, 2009). Of course, many smaller and larger particles occur within the flow. The particles exist in a continual state of flux; they can break or they can combine to form particle agglomerates, especially in the runout zone where the terrain flattens and the flow becomes slower. Air mixed with ice dust is blown out of the core to form the suspension layer. Both small granules and ice dust are blown out of the avalanche core as well. However, the smaller granular aggregates are not suspended, but, once ejected from the core, will return rapidly to flow. The granular aggregates can occur high above the ground (10–20 m) increasing the height of the zone where large, but local, impact pressures can be exerted on tall structures, including trees. Because heavier particles fall out of the dust cloud, this region of the avalanche core is sometimes termed the *segregation layer*. These aspects of the flow core are a result of the fact that the upper surface of the avalanche is essentially a free surface.

The denser regions within the avalanche core also exhibit significant variations in bulk flow density (Gauer et al., 2008). Because of several factors (ground roughness, terrain undulations, large overburden pressures, and the braking effects of snow cover deconstruction and entrainment), granules at the running surface move slower than granules in the upper region of the flow. Measured velocity profiles have been reported in Kern et al. (2009). Velocity gradients indicate not only granular collisions and thus frictional dissipation, but also strong dilatative movements within the avalanche core (Buser and Bartelt, 2011). This causes an expansion of the avalanche flow volume and therefore a decrease in bulk avalanche flow density. The degree of volume expansion depends on the avalanche flow height. It is harder to change the flow volume of larger flow heights where the overburden pressures are larger. At the front of the avalanche, where flow heights are small and frictional forces are large, strong expansion movements can occur within the avalanche core.

12.4.4 The suspension cloud

If the avalanche snow is dry, ice grains (ice dust) become suspended in the surrounding air to form a "powder" or "suspension" cloud. The dust can arise from a layer of weakly bonded fresh snow, or the abrasive granular interactions between dry-snow granules within the avalanche. Mean grain sizes are 0.1 mm (Rastello et al., 2011). The ice dust is mixed with air in the avalanche core and blown out of the avalanche, often in violent vertical movements to form irregular plume-like structures. The plumes are formed at different locations and rise at different speeds; the stronger plumes will often rise and spread more quickly, spreading over and consuming slower rising plumes. The powder cloud surface is therefore uneven and composed of billows and clefts. This gives powder avalanches their distinctive turbulent appearance.

Japanese measurements of powder cloud densities from pressure measurements reveal bulk densities between 3 and 5 kg/m^3 (Nishimura et al., 1993). Although these densities appear low, they are more than enough to give powder clouds their opaque gray-white color. A cubic meter of powder cloud dust will contain some 10,000,000 ice particles. This is enough to obstruct the view of the avalanche core flowing below. It hinders a clear understanding of the powder cloud formation process.

Using stereogrammetric, georeferenced photo images of the powder cloud at the Swiss Vallée de la Sionne test site, it has been possible to measure the total volume of powder clouds. These are immense. For avalanches consisting of 50,000–100,000 m^3 of flowing snow debris, the powder cloud volumes can exceed 10,000,000 m^3. The powder cloud volume can be well over 100 times the volume of the core. The suspension ratio (the ratio of powder mass to core mass) is estimated to be between 5% and 20%. This is an indication of the large amount of air entrained by the powder cloud.

Another use of stereogrammetric imaging is to trace the movement of plumes (Fig. 12.15). This reveals that the plumes are primarily created at the front and edges of the flow. The plumes quickly decelerate and become stationary, sometimes only a 100 m behind the leading edge of the avalanche. This is an indication of large drag forces acting on the cloud. These drag forces arise from air entrainment and drag as the particles are expelled into the surrounding air. The front of the cloud is moving faster than the tail, or wake of the cloud. The movement of the powder cloud resembles the smoke blown out by a steam engine; that is, there is a continual creation of new powder at the avalanche front that becomes stationary as the avalanche moves forward. The motion of the cloud does not resemble a rigid body movement (in which the front and rear move at the same speed) as some powder snow avalanches models would suggest (Ancey, 2004; Beghin and Olagne, 1991).

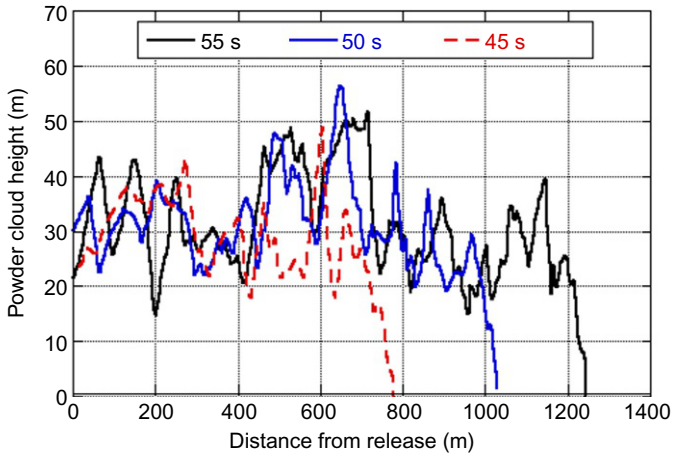

FIG. 12.15

Cross section of measured powder cloud heights of a Vallée de la Sionne avalanche for three times: $t = 45$, 50, and 55 s. The heights reach over 50 m. The cloud is created at the front of the avalanche. The plumes initially move forward but are almost stationary 100 m behind the avalanche front.

12.4.5 Snow entrainment

Observations reveal that avalanches can entrain snow layers, typically a layer of fresh snow. Wet-snow avalanches frequently remove the entire snowpack exposing the ground and creating muddied depositions (Jomelli and Bertran, 2001). In fact, avalanches play an important role in transporting debris (soil, rocks, deadwood) from the starting zone to the runout zone (Bozhinskiy and Losyev, 1998; Swift et al., 2021).

Entrainment processes are usually divided into three phenomenological categories (Cherepanov and Esparragoza, 2008; Gauer and Issler, 2004; Sovilla, 2004): (1) frontal plowing, (2) basal erosion, and (3) snow layer fracture entrainment.

Snow entrainment affects avalanche motion in four ways: (1) it changes the overall mass balance of the avalanche; (2) it can change the temperature and moisture content of the flowing snow, and therefore snow entrainment can change the avalanche flow regime from dry to wet, or from dilute to dense; (3) as the avalanches runs over the snow cover, it produces internal shear gradients in the avalanche core and therefore entrainment can enhance the production of chaotic and vertical motions (granular fluctuations and rotations), especially at the front of the avalanche; and (4) dry snow covers are a good source of ice dust that is subsequently mixed with the air blown out of the avalanche core to create the suspension cloud of powder snow avalanches.

Avalanche flow volume and avalanche mobility are related: In general, observations reveal that larger avalanches have longer runout distances (Bozhinskiy and Losyev, 1998). This fact is reflected in calculation guidelines where larger (extreme) avalanches are assigned lower friction values. Theoretically, this indicates that snow entrainment should positively affect avalanche mobility. At present, however, no physical explanation exists as to why this should occur. In fact, many experts maintain that entrainment will slow the avalanche down and reduce runout distances because accelerating the entrained snow to the avalanche velocity, breaking the snow cover, or snow cover plowing consumes avalanche flow energy. In practice the effect of avalanche entrainment is handled simply by using extreme (and therefore low) friction values for large avalanches, without actual consideration of the entrained mass.

More advanced avalanche dynamics models consider not only the entrained mass, but also the entrained heat energy (temperature) and moisture content (Vera Valero et al., 2015). This modifies the internal energy fluxes in the avalanche core. That is, even after the energy losses of entrainment are accounted for, an increase in mobility occurs due to flow regime transitions induced by the production of random energy (more dilute flows), or meltwater lubrication (temperature effects), or enhanced moisture content (reduced shear resistance) (Bartelt et al., 2012c). Clearly, entrainment has a much greater effect on avalanche flow then simply increasing the flow mass.

12.4.6 Stopping and depositional features

A better understanding of how avalanches stop is being driven by new methods to measure avalanche deposits, particularly by accurate terrestrial and airborne laser scanning techniques (Bartelt et al., 2012b; Bühler et al., 2009). Increasingly accurate and handheld GPS devices are useful to trace the extent of avalanche deposits in field investigations. Because modern avalanche dynamics models predict the distribution of mass in the runout zone, increased interest exists to compare measured and calculated runout distances, as well as calculated and measured deposition heights (Christen et al., 2010).

Avalanche deposition patterns are strongly dependent on three-dimensional terrain characteristics (roughness, steepness of runout zone, counter slope, terrain undulations, gullies, etc.) and therefore are ideal to test the stopping mechanics of avalanche dynamics models (Gauer, 2014, 2018). Often, information gathered from avalanche deposits is the only hard evidence available to reconstruct an avalanche event.

Stopping is driven by the imbalance between the driving gravitational forces G and shear friction S. The point where avalanche deceleration begins is usually estimated to be given at the point P where the tangent of the slope angle φ_P is equal to the value of the Coulomb friction μ:

$$\tan(\varphi_P) = \mu$$

This is a useful formula as most avalanche dynamics models rely on some kind of Coulomb friction to describe when an avalanche stops, i.e.:

$$\frac{S}{N} = \mu$$

where S is shear and N is the normal pressure exerted by the avalanche on the basal running surface. Avalanches can begin to decelerate on steep slopes between $\mu \approx 0.25$ and 0.45 (Sovilla et al., 2010). For far-reaching (extreme) avalanches, different investigators have found values between $\mu \approx 0.12$ and 0.15 (e.g., Bozhinskiy and Losyev, 1998; Salm et al., 1990). Even smaller values have been observed in practice. The formula is well tested and facilitates a simple, direct approximation of runout distance.

Actual shear and normal force measurements in snow chute experiments (Platzer et al., 2007) reveal that avalanche friction cannot be well described by a constant μ. It appears that avalanche friction varies over the length of the avalanche (it is lowest at the front of the avalanche and increases toward the tail). Other factors, including snow temperature and moisture content, can also influence μ. Interestingly, snow chute experiments show that the shear S can have different values for the same normal pressure N. The fact that μ can vary—it is a frictional process, rather than a frictional constant—explains the tremendous variation in "calibrated" friction parameters used to model snow avalanches. Because this frictional process is mass dependent, smaller avalanches can stop on steeper slopes, giving the impression that smaller avalanches have higher friction values.

How the friction μ evolves over time determines the distribution of depositions in the runout zone. If the terrain permits, avalanche deposits can be very regular. A tendency exists for higher deposition heights at lower slope angles. However, avalanche deposits can be highly irregular and exhibit four unique features (Bartelt et al., 2012b):

1. *Levees and sidewall-type constructions* (Fig. 12.16A and B). Levees commonly occur in wet-snow avalanche deposits. They arise when avalanche snow stops flowing at the outer boundaries of an avalanche. The interior flow continues to move forward, and internal shear planes are created several meters inward from the stopped outer boundary. As the interior flow drains, it leaves the sidewalls exposed, creating channel-like structures in the depositions. Levees are an indication of strong internal friction gradients within the flow. Although these friction gradients can be induced by terrain undulations, levees are also found on flat and relatively homogeneous runout zones, indicating that levee formation is triggered by internal variations of avalanche velocity (the velocity is smaller at the outer edges of the flow). Levees can form at the front of slow-moving (wet-snow) avalanches, or at the slow-moving tail of dry-snow flowing avalanches. The importance of levee sidewalls is that they can be large (over 5 m in height) and thus form structures that can deflect the

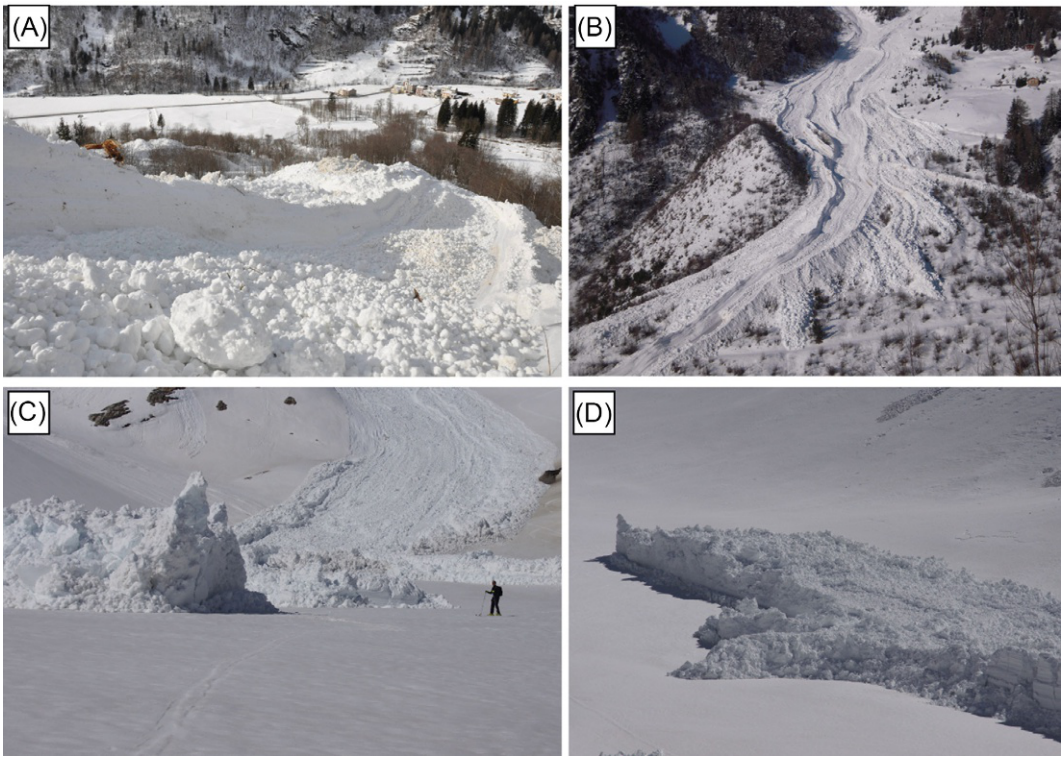

FIG. 12.16

Different avalanche deposition types: (A) levee with sidewalls; (B) levee; (C) avalanche flow finger with pileup; and (D) avalanche flow finger.

From Bartelt, P., Glover, J., Feistl, T., Bühler, Y., Buser, O., 2012b. Formation of levees and en-echelon shear planes during snow avalanche run-out. J. Glaciol. 58(211), 980–992.

flowing mass of the same avalanche, or subsequent avalanches on the same avalanche track (Fig. 12.16B).

2. *Avalanche flow fingers* (Fig. 12.16C and D). Avalanche flow fingers often extend beyond the reach of the bulk of deposited avalanche mass. Typically, they are narrow structures (5–10 m in width; see Fig. 12.16D), but they can also be rather wide depositional lobes (up to 50 m, say). Flow fingers typically arise in moist or wet-type avalanches and are an indication of strong preferential flow behavior. The flow fingers can follow roads or other terrain features (gullies). The sides of flow fingers are steep, signifying strong cohesive properties of the flowing snow. In a sense they are similar to the interior flow of a self-formed levee channel, except that the mass at the outer boundaries does not stop and builds no sidewalls. Flow fingers are a problem for avalanche runout calculations as they are difficult to predict. The flow fingers can bend 90 degrees or more.
3. *Shear planes and en echelon shear faults*. Both vertical and horizontal shear planes occur in avalanche deposits. Vertical planes, parallel to the flow direction, occur on levee sidewalls.

Horizontal (or basal) shear planes are formed as the avalanche moves in a plug-like motion over terrain undulations. Snow fills in the undulations and acts to smooth the terrain. Commonly the basal shear planes are formed in the avalanche interior between levee sidewalls. Frictional rubbing can produce heat that, depending on the initial temperature of the snow, can melt the frictional surfaces of avalanching snow. The meltwater usually refreezes. This hardens the sheared surface, giving it a shiny appearance that is visible from a considerable distance. Because of the evolution of flow friction, avalanches do not stop at once: The avalanche tail can stop first, behind the front. This leads to the formation of en echelon-type fault structures in which the front is "pulled" away from the tail.

4. *Pileups* (Fig. 12.16C). Avalanche pileups can occur at the end of levee-type channels, or they can occur at steep slope transitions, for example, at the exit of a gully at the beginning of a flat runout zone. Avalanche snow can also pile up at the transition between a slope and steep counter slope. Avalanche pileups are dangerous depositional features because they can be very high (over 20 m) and therefore change the topography of the avalanche track.

12.4.7 Avalanche interaction with obstacles

The problem of how to adequately design buildings and other structures that stand in the path of an avalanche is central to hazard mapping and the planning of mitigation measures. Real-scale experiments in Switzerland, Russia, and Canada show that avalanches can exert immense pressures on obstacles (Bozhinskiy and Losyev, 1998; McClung and Schaerer, 1985; Sovilla et al., 2008). The obstacles (measurement pylons) are regarded as stationary, rigid bodies in comparison with the fluidlike behavior of the avalanche body, which can flow around or completely immerse the obstacle. Obstacle interaction is therefore not only an impact phenomenon but lasts significantly longer as the avalanche flows past the obstacle. Engineers are mostly interested in the maximum pressure and pressure distribution, as this determines both the dynamic forces and overturning moments exerted on the structure.

Maximum pressures of 100 t/m^2 have been measured at the Swiss Vallée de la Sionne test site (Fig. 12.17); Russian researchers have reported pressures of up to 200 t/m^2 (Bozhinskiy and Losyev, 1998). Several dry-mixed flowing avalanches recorded at Vallée de la Sionne site have exerted peak pressures between 20 and 50 t/m^2 when traveling at speeds between 30 and 40 m/s. Pressure signals can be both intermittent and continuous functions in time, depending on the avalanche flow regime (dispersed, dense) and type (wet, dry). A problem with the analysis of pressure signals is that different measurement techniques can measure different pressures at different periods during the passage of the avalanche.

Pressure models of avalanche-obstacle interaction assume that the avalanche body is a continuum. Pressures p can be evaluated using the hydrodynamic formula:

$$p = c\frac{1}{2}\rho U^2$$

where c is the dimensionless coefficient of resistance, dependent on the shape of the object ($c = 1$ for slender objects; $c = 2$ for wider, wall-like structures). A prerequisite for a pressure analysis is an estimate of the avalanche speed U and bulk flow density ρ. It is necessary to have an idea of the avalanche flow height to determine the height of the applied pressure.

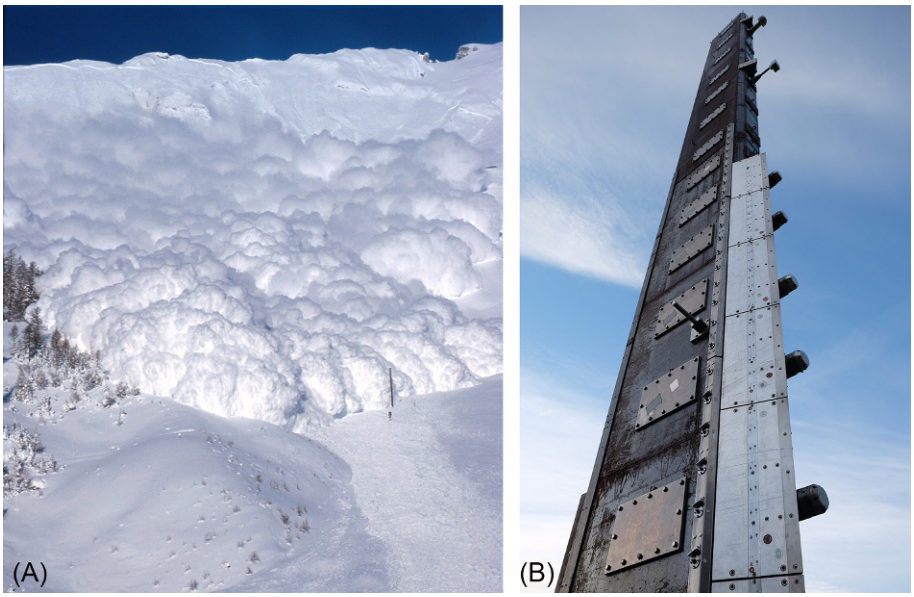

FIG. 12.17

Avalanche dynamics experimental site Vallée de la Sionne (Arbaz, Switzerland). (A) Very large dry-mixed flowing avalanche that was artificially triggered by explosives. The avalanche front is about to hit the measurement pylon, which is 20 m high. (B) Oval-shaped measurement pylon to record pressures, velocities, densities, temperatures, and flow depth at different heights in the avalanche flow.

Photography: SLF; M. Hiller.

As we have seen, snow avalanches consist of hard snow granules (as well as rocks and deadwood) and will undergo significant variations in the bulk flow density. The application of the continuum formula is therefore questionable since it does not take into account the granular nature of the flow. The formula

$$p_g = \frac{4}{3}\rho_g U^2$$

can be used to predict local, granule impact pressures. The formula assumes the time of a granule collision is $t = d/2U$, where d is the diameter of the granule. It assumes a plastic collision in which the granule is completely destroyed at impact. Our experience with this formula is that it well approximates measured impact pressures, which are often performed with pressure cells of size d. The granule density ρ_g varies between 400 and 500 kg/m^3, indicating significant densification of the snow during flow.

12.5 Avalanche mitigation

To avoid avalanche disasters, first of all, potential avalanche terrain and accordingly a potential avalanche problem need to be recognized. Indications include oral and written history of previous avalanche events, vegetation clues and snow-depth records, and most importantly, terrain. A terrain

analysis can be done by identifying all areas steeper than about 30 degrees by using a GIS and a DTM. Obviously, any infrastructure in these potential starting zones is endangered. The next step, the risk analysis, involves assessing the frequency, magnitude, and runout of avalanches initiating from the identified potential starting zones (e.g., Schweizer, 2004).

Depending on the object endangered and the frequency and size of potential avalanches, the resulting risk is too high and mitigation measures are planned. If residential areas or areas where development is planned are endangered, land-use planning measures should be established, based on the hazard map, so that buildings in hazard zones are avoided, restricted, or designed to withstand potential avalanche pressures. In Switzerland, for example, hazard zones are defined based on avalanche frequency and impact pressure. For residential areas, large avalanches with return periods as high as 300 years need to be taken into account. For roads, return periods are typically much shorter, up to several times a year. If a road is endangered by several potentially large avalanches with return periods of less than 10 years, an active avalanche control program (including the use of explosives) and/or the construction of snow sheds should be considered (Fig. 12.18). If the avalanches potentially hitting the road are rather small and/or infrequent, temporary closures based on an avalanche forecast may be the adequate protection measure (Jamieson et al., 2002). For highly endangered infrastructure (highways, railways,

FIG. 12.18

Avalanche mitigation measures include snow sheds (protecting the railway line), deflecting dams (protecting the Trans-Canada Highway) and warning signs that reduce the risk by reducing the exposure (Field, BC, Canada).

Photography: J. Schweizer.

mining operations, ski areas, etc.), local forecasting services need to be established that also run the avalanche control program (e.g., Hendrikx et al., 2005; Schweizer et al., 1998).

The various mitigation measures should be applied, usually in combination, in a coordinated manner to reduce the avalanche risk to an acceptable level. This approach is known as integral risk management (Wilhelm et al., 2001). In general, mitigation measures are grouped into temporary (or short-term) and permanent (or long-term) measures, both of which can be subdivided into either active (e.g., preventing avalanche release by snow-supporting structures) or passive measures (e.g., establishing hazard maps). The various mitigation measures are described in more detail by, for example, Bründl and Margreth, (2021), McClung and Schaerer (2006), and Rudolf-Miklau et al. (2015).

12.6 Avalanche forecasting

Avalanche forecasting was described by McClung (2002) as the prediction of snow instability in space and time relative to a given triggering level. The main sources of uncertainty in forecasting are the unknown temporal evolution and the spatial variations of instability in the snow cover. In the framework of integral risk management, avalanche forecasting is considered a short-term, passive mitigation measure. Snow avalanches are the only natural hazard—apart from some purely meteorological hazards such as storms and heavy precipitation—that can be forecast.

Snow avalanche prediction (forecasting snowpack instability) can be made for various scales (McClung and Schaerer, 2006). We will focus on the regional scale (1000 km^2), the local scale (100 km^2), and the scale of an individual avalanche path (1 km^2). Typically, the prediction is about the danger level, the avalanche activity (or occurrence), and the probability of the single event for these three scales, respectively. In avalanche forecasting, a mismatch commonly occurs between the scale of the forecast and the scale of the underlying data (Hägeli and McClung, 2004).

Today, most countries with areas where people and infrastructure are significantly endangered by avalanches operate an avalanche forecasting service, similar to a weather service, which issues warnings, or so-called avalanche bulletins. These services primarily forecast the regional avalanche danger by describing the hazard situation with one of five degrees of danger: *5—Very High* (or *Extreme* in North America); *4—High*; *3—Considerable*; *2—Moderate*; and *1—Low* (Table 12.3). The avalanche danger level is defined in terms of snowpack stability, the spatial distribution of snowpack stability (i.e., the frequency of snowpack weaknesses where avalanche may originate from), and potential avalanche size (e.g., Meister, 1995; Statham et al., 2018). All three elements are supposed to be combined when assigning a danger level to a given avalanche situation (Schweizer et al., 2020). However, they do not have the same weight. Recent analyses suggest that avalanche size is of secondary importance compared to snowpack stability and its distribution when assessing the danger level (Techel et al., 2020).

Operational avalanche forecasting mainly relies on meteorological observations and forecasts in combination with snow cover instability observations, ideally direct observations of avalanches (McClung and Schaerer, 2006). It involves the assimilation of multiple data sources to make predictions over complex interacting processes. For many decades now, avalanche professionals have developed successful decision-making strategies to deal with this complexity (LaChapelle, 1980). These rule-based empirical strategies, sometimes applied intuitively, are able to deal with many of the numerous processes and scales involved in avalanche formation. However, the employed methods

Table 12.3 Example of avalanche danger scale as used by most avalanche forecasting services. The five-degree danger scale was originally introduced by the European warning services in 1994.

North American Public Avalanche danger scale

Avalanche danger is determined by the likelihood, size and distribution of avalanches

Danger level		Travel advice	Likelihood of avalanches	Avalanche size and distribution
5 Extreme		Avoid all avalanche terrain	Natural and human-triggered avalanches certain	Large to very large avalanches in many areas
4 High		Very dangerous avalanche conditions. Travel in avalanche terrain not recommended	Natural avalanches likely; human-triggered avalanches very likely	Large avalanches in many areas; or very large avalanches in specific areas
3 Considerable		Dangerous avalanche conditions. Careful snowpack evaluation, cautious route-finding and conservative decision-making essential	Natural avalanches possible; human-triggered avalanches likely	Small avalanches in many areas; or large avalanches in specific areas; or very large avalanches in isolated areas
2 Moderate		Heightened avalanche conditions on specific terrain features. Evaluate snow and terrain carefully; identify features of concern	Natural avalanches unlikely; human-triggered avalanches possible	Small avalanches in specific areas; or large avalanches in isolated areas
1 Low		Generally safe avalanche conditions. Watch for unstable snow on isolated terrain features	Natural and human-triggered avalanches unlikely	Small avalanches in isolated areas or extreme terrain

Safe backcountry travel requires training and experience. You control your own risk by choosing where, when and how you travel.

are largely based on experience of the forecaster and are therefore prone to subjectivity, unable to deal with unusual situations, and difficult to transfer to new personnel. Recently, rule-based decision support tools have been developed for recreationists that relate terrain to the danger level (see McCammon and Hägeli, 2007). However, these tools often fail to consider the consequences in the risk assessment process (Reuter and Semmel, 2018).

Numerous attempts have been made to develop objective avalanche forecasting techniques. Such efforts predominantly consist of statistically relating local weather observations to avalanche occurrence data or estimated avalanche danger. Statistical forecasting models are based on the idea that similar weather conditions lead to comparable avalanche situations. Various methods have been used, including linear regression analysis, multivariate discriminant analysis, time-series analysis, nearest neighbors, or pattern recognition techniques (e.g., Buser, 1983; Pozdnoukhov et al., 2011; Schweizer and Föhn, 1996). Depending on the scale of the study area and the quality of the input data, the accuracy of the statistical models can vary greatly. A major drawback is the poor temporal resolution of avalanche observations or estimated avalanche danger. Therefore, coarse-scale meteorological parameters, such as the amount of new snow in the last 24, 48, or 72 h, are typically used as input parameters (McClung and Tweedy, 1994). High-frequency meteorological data (e.g., recorded at 30-min intervals) or forecasts, which nowadays are widely available, cannot therefore be exploited to their fullest extent. With recent advances in avalanche detection systems, higher resolution avalanche data may soon become available (Heck et al., 2019b; Mayer et al., 2020; Schimmel et al., 2017).

Another shortcoming of most statistical forecasting models is the failure to include quantitative snowpack stratigraphy data (e.g., Schweizer and Föhn, 1996). Such snowpack data are important for avalanche forecasting, especially during periods of low avalanche activity and stable weather conditions. In fact, snow avalanches are the only hazard where in situ tests exist that can provide information on the state of instability. Of course, these tests provide point information only that needs to be extrapolated—a task hampered by the inherently variable nature of the mountain snowpack (Reuter et al., 2016). A first step toward a more deterministic approach to avalanche forecasting (which would include simulating avalanche release) therefore consists of modeling snowpack characteristics and deriving stability information.

Essentially two types of numerical models exist: one-dimensional snow cover models and three-dimensional model systems. One-dimensional models, such as CROCUS (Brun et al., 1992; Vionnet et al., 2012) and SNOWPACK (Bartelt and Lehning, 2002; Lehning et al., 2002a,b), compute the snow cover stratigraphy by solving the one-dimensional mass and energy balance equations using meteorological data as input. The modeled stratigraphy can then be interpreted with regard to stability (e.g., Monti et al., 2014; Schweizer et al., 2006; Vernay et al., 2015). Alternatively, modeled snow stratigraphy variables can be used as input variables to improve the performance of statistical avalanche forecasting models (Schirmer et al., 2009). A limitation of one-dimensional models is the lack of spatial snow-cover information.

Such information is provided by three-dimensional model systems, such as SAFRAN-CROCUS-MEPRA (SCM) (Coléou et al., 2009; Durand et al., 1999) and Alpine3D, which includes SNOWPACK (Lehning et al., 2006). These model systems use spatial meteorological input data and account for three-dimensional processes such as radiation redistribution and snow transport by wind. A large part of the complexity was removed in the French SCM model chain by providing automated avalanche danger prediction for virtual slopes. It is the only real operational forecasting model on the basis of physical modeling. However, given the overall complexity of the interactions between the snowpack and meteorological parameters and the high spatial resolution required, surface process model systems are very computationally intensive and many uncertainties still remain. Furthermore, interpretation of spatial snow cover data with regard to snow slope stability remains an open issue (Bellaire et al., 2018).

Field observations on snow stratigraphy are widely used to investigate snow cover instability for avalanche forecasting (e.g., Schweizer and Jamieson, 2010b). Over the last decade, new in situ measurement techniques have been developed to objectively describe the stratigraphy of a natural snowpack, including near-infrared photography (Matzl and Schneebeli, 2006), the snow micropenetrometer (SMP; Schneebeli and Johnson, 1998), contact spectrometry (Painter et al., 2007), and upward-looking ground-penetrating radars (Schmid et al., 2014). Although these methods primarily provide new insight into the microstructure of snow and its physical processes, interpretation of the data remains complicated, in particular with regard to snow stability (e.g., Bellaire et al., 2009; van Herwijnen et al., 2009). Recently, promising advances have been made by combining microtomography and SMP measurements (Reuter et al., 2019). Moreover, snow instability modeling based on SMP data showed promising results (Reuter et al., 2015), demonstrating the importance of considering both failure initiation and crack propagation. Nevertheless, manual snow cover measurements, consisting of snow profiles and snow stability tests, presently remain the method of choice for avalanche forecasting. Snow cover observations are typically compared to observed avalanche activity or estimated avalanche danger to obtain empirical relationships (e.g., Schweizer and Jamieson, 2007; van Herwijnen and Jamieson, 2007). Although these in situ tests have a number of deficiencies, including an error rate of at least

5%–10%, correlations between manual snow cover measurements and snow slope stability have been identified (Schweizer and Jamieson, 2010b). With the advent of the propagation saw test (PST) and the development of a model to derive the critical crack length, which is measured in the PST, a snow instability metric exists that allows for easy comparison between measurement and model (Richter et al., 2019; Schweizer et al., 2016b).

In general, prediction requires predictability, that is, some sort of a precursor, or observational variable that announces the event. In the case of snow avalanches, avalanche prediction during storms is mainly based on precipitation amounts; new snow is considered as precursor. Obviously, precursors more related to the state of the snowpack would be useful. Pioneering work in the 1970s tried to relate acoustic emissions from a natural snow cover to avalanche formation and slope stability (e.g., Gubler, 1979; Sommerfeld, 1977; St. Lawrence and Bradley, 1977). Given the differences in instrumental setup and the lack of a thorough description of the field experiments, in particular with regard to the signal processing and the treatment of environmental background noise, results from early microseismic studies remain ambiguous.

Whereas laboratory measurements on snow failure have indicated that monitoring acoustic emissions may reveal imminent failure, applying the technique in the field is difficult due to strong attenuation of high-frequency signals in snow (Reiweger and Schweizer, 2013a). Alternatively, seismic sensors can be used, but van Herwijnen and Schweizer (2011b) were unable to detect precursors to slab avalanche release. However, the avalanche occurrence data (van Herwijnen and Schweizer, 2011a) suggest that avalanches could be used as precursors because often at the beginning of periods of significant avalanche activity the number of events increases (Schweizer and van Herwijnen, 2013). Obviously, direct observations of avalanches are the most reliable evidence of unstable snow conditions and of fundamental importance for avalanche forecasting.

12.7 Concluding remarks

Disasters due to snow avalanches have caused the loss of life and property damage in most populated snow-covered mountain areas. Although in the past people had primarily to rely on experience, which is known to be of limited value when dealing with rare and extreme events such as large snow avalanches, today advanced methods exist that enable recognition of the risk as well as its mitigation. Still, this does not mean that disasters due to snow avalanches will no longer occur. Even with modern monitoring and modeling methods, it is not possible to predict the exact location and time of an avalanche release—primarily due to the lack of reliable precursors and the inherently variable nature of the mountain snowpack. Clearly, physics-based numerical models are helpful tools to predict avalanche motion and impact, but uncertainties remain despite major advances—not least in view of the uncertain consequences of climate change as both air temperature and precipitation, including its intensity, may increase; so far no clear direction of trend for avalanche activity in the future has been found (IPCC, 2019). Even after applying mitigation measures, a residual risk remains because completely reducing the risk is definitely not cost-efficient. Therefore, combining permanent and temporary protection measures is most promising, but requires that the risk is actively managed. By doing so, the risk to people—living, traveling, or recreating in the mountains—can effectively be reduced to an acceptable level.

References

Ancey, C., 2004. Powder snow avalanches: approximation as non-Boussinesq clouds with a Richardson number-dependent entrainment function. J. Geophys. Res. 109, F01005.

Ancey, C., Gervasoni, C., Meunier, M., 2004. Computing extreme avalanches. Cold Reg. Sci. Technol. 39 (2–3), 161–180.

BABS, 2003. KATARISK. Katastrophen und Notlagen in der Schweiz. In: Eine Risikobeurteilung aus der Sicht des Bevölkerungsschutzes. Bundesamt für Bevölkerungsschutz BABS (Swiss Federal Office for Civil Protection FOCP), Bern, Switzerland. 83 pp.

Baggi, S., Schweizer, J., 2009. Characteristics of wet snow avalanche activity: 20 years of observations from a high alpine valley (Dischma, Switzerland). Nat. Hazards 50 (1), 97–108.

Bartelt, P., Lehning, M., 2002. A physical SNOWPACK model for the Swiss avalanche warning; part I: numerical model. Cold Reg. Sci. Technol. 35 (3), 123–145.

Bartelt, P., McArdell, B.W., 2009. Granulometric investigations of snow avalanches. J. Glaciol. 55 (193), 829–833.

Bartelt, P., Buser, O., Platzer, K., 2006. Fluctuation-dissipation relations for granular snow avalanches. J. Glaciol. 52 (179), 631–643.

Bartelt, P., Meier, L., Buser, O., 2011. Snow avalanche flow-regime transitions induced by mass and random kinetic energy fluxes. Ann. Glaciol. 52 (58), 159–164.

Bartelt, P., Feistl, T., Bühler, Y., Buser, O., 2012a. Overcoming the stauchwall: viscoelastic stress redistribution and the start of full-depth gliding snow avalanches. Geophys. Res. Lett. 39.

Bartelt, P., Glover, J., Feistl, T., Bühler, Y., Buser, O., 2012b. Formation of levees and en-echelon shear planes during snow avalanche run-out. J. Glaciol. 58 (211), 980–992.

Bartelt, P., Vera, C., Steinkogler, W., Feistl, T., Buser, O., 2012c. The role of thermal temperature in avalanche flow. In: Proceedings ISSW 2012. International Snow Science Workshop, Anchorage AK, U.S.A., 16–21 September 2012, pp. 32–37.

Beghin, P., Olagne, X., 1991. Experimental and theoretical study of the dynamics of powder snow avalanches. Cold Reg. Sci. Technol. 19 (3), 317–326.

Bellaire, S., Pielmeier, C., Schneebeli, M., Schweizer, J., 2009. Stability algorithm for snow micro-penetrometer measurements. J. Glaciol. 55 (193), 805–813.

Bellaire, S., van Herwijnen, A., Mitterer, C., Schweizer, J., 2017. On forecasting wet-snow avalanche activity using simulated snow cover data. Cold Reg. Sci. Technol. 144, 28–38.

Bellaire, S., van Herwijnen, A., Bavay, M., Schweizer, J., 2018. Distributed modeling of snow cover instability at regional scale. In: Fischer, J.-T., Adams, M., Dobesberger, P., Fromm, R., Gobiet, A., Granig, M., Mitterer, C., Nairz, P., Tollinger, C., Walcher, M. (Eds.), Proceedings ISSW 2018. International Snow Science Workshop, Innsbruck, Austria, 7–12 October 2018, pp. 871–875.

Bobillier, G., Bergfeld, B., Capelli, A., Dual, J., Gaume, J., van Herwijnen, A., Schweizer, J., 2020. Micromechanical modeling of snow failure. Cryosphere 14 (1), 39–49.

Bozhinskiy, A.N., Losyev, K.S., 1998. The fundamentals of avalanche science. In: Mitteilungen des Eidg. vol. 55. Instituts für Schnee-und Lawinenforschung SLF, Davos, Switzerland. 280 pp.

Brun, E., David, P., Sudul, M., Brunot, G., 1992. A numerical model to simulate snow-cover stratigraphy for operational avalanche forecasting. J. Glaciol. 38 (128), 13–22.

Bründl, M., Bartelt, P., Schweizer, J., Keiler, M., Glade, T., 2010. Review and future challenges in snow avalanche risk analysis. In: Alcantara-Ayala, I., Goudie, A.S. (Eds.), Geomorphological Hazards and Disaster Prevention. Cambridge University Press, New York, USA, pp. 49–61.

Bründl, M., Margreth, S., 2021. Integrative risk management: the example of snow avalanches. In: Haeberli, W., Whiteman, C. (Eds.), Snow and Ice-Related Hazards, Risks and Disasters. Elsevier, pp. 259–296.

Bühler, Y., Hüni, A., Christen, M., Meister, R., Kellenberger, T., 2009. Automated detection and mapping of avalanche deposits using airborne optical remote sensing data. Cold Reg. Sci. Technol. 57 (2–3), 99–106.
Bühler, Y., Kumar, S., Veitinger, J., Christen, M., Stoffel, A., Snehmani, 2013. Automated identification of potential snow avalanche release areas based on digital elevation models. Nat. Hazards Earth Syst. Sci. 13 (5), 1321–1335.
Bühler, Y., von Rickenbach, D., Stoffel, A., Margreth, S., Stoffel, L., Christen, M., 2018. Automated snow avalanche release area delineation—Validation of existing algorithms and proposition of a new object-based approach for large-scale hazard indication mapping. Nat. Hazards Earth Syst. Sci. 18 (12), 3235–3251.
Buser, O., 1983. Avalanche forecast with the method of nearest neighbours: an interactive approach. Cold Reg. Sci. Technol. 8 (2), 155–163.
Buser, O., Bartelt, P., 2009. Production and decay of random kinetic energy in granular snow avalanches. J. Glaciol. 55 (189), 3–12.
Buser, O., Bartelt, P., 2011. Dispersive pressure and density variations in snow avalanches. J. Glaciol. 57 (205), 857–860.
CAA, 2016. In: Campbell, C., Conger, S., Gould, B., Haegeli, P., Jamieson, B., Statham, G. (Eds.), Technical Aspects of Snow Avalanche Risk Management—Resources and Guidelines for Avalanche Practitioners in Canada. Canadian Avalanche Association, Revelstoke, BC, Canada. 117 pp.
Caduff, R., Wiesmann, A., Bühler, Y., Pielmeier, C., 2015. High spatial and temporal resolution continuous monitoring of snowpack displacement with terrestrial radar interferometry. Geophys. Res. Lett. 42 (3), 813–820.
Capelli, A., Reiweger, I., Schweizer, J., 2018. Acoustic emissions signatures prior to snow failure. J. Glaciol. 64 (246), 543–554.
Ceaglio, E., Mitterer, C., Maggioni, M., Ferraris, S., Segor, V., Freppaz, M., 2017. The role of soil volumetric liquid water content during snow gliding processes. Cold Reg. Sci. Technol. 136, 17–29.
Chandel, C., Mahajan, P., Srivastava, P.K., Kumar, V., 2014. The behaviour of snow under the effect of combined compressive and shear loading. Curr. Sci. 107 (5), 888–894.
Cherepanov, G.P., Esparragoza, I.E., 2008. A fracture-entrainment model for snow avalanches. J. Glaciol. 54 (184), 182–188.
Christen, M., Kowalski, J., Bartelt, P., 2010. RAMMS: numerical simulation of dense snow avalanches in three-dimensional terrain. Cold Reg. Sci. Technol. 63 (1–2), 1–14.
Clarke, J.A., McClung, D.M., 1999. Full-depth avalanche occurrences caused by snow gliding. Coquihalla, B.C., Canada. J. Glaciol. 45 (151), 539–546.
Coléou, C., Giraud, G., Daniélou, Y., Dumas, J.-L., Gendre, C., Pougatch, E., 2009. Use of the models Safran-Crocus-Mépra in operational avalanche forecasting. In: Schweizer, J., van Herwijnen, A. (Eds.), International Snow Science Workshop ISSW, Davos, Switzerland, 27 September–2 October 2009. Swiss Federal Institute for Forest, Snow and Landscape Research WSL, pp. 341–345.
Conlan, M.J.W., Jamieson, B., 2016. Formation and strengthening of layers of dry faceted crystals above artificial melt-freeze crusts from overburden stress in a controlled environment. Can. Geotech. J. 53 (2), 187–195.
Dreier, L., Harvey, S., van Herwijnen, A., Mitterer, C., 2016. Relating meteorological parameters to glide-snow avalanche activity. Cold Reg. Sci. Technol. 128, 57–68.
Durand, Y., Giraud, G., Brun, E., Mérindol, L., Martin, E., 1999. A computer-based system simulating snowpack structures as a tool for regional avalanche forecasting. J. Glaciol. 45 (151), 469–484.
EAWS, 2020. Avalanche Size. https://www.avalanches.org/standards/avalanche-size/. (Accessed 5 December 2020).
Endo, Y., 1985. Release mechanism of an avalanche on a slope covered with bamboo bushes. Ann. Glaciol. 6, 256–257.
Fierz, C., Armstrong, R.L., Durand, Y., Etchevers, P., Greene, E., McClung, D.M., Nishimura, K., Satyawali, P.K., Sokratov, S.A., 2009. The International Classification for Seasonal Snow on the Ground. HP-VII Technical Documents in Hydrology. vol. 83 UNESCO-IHP, Paris, France. 90 pp.

Gauer, P., 2014. Comparison of avalanche front velocity measurements and implications for avalanche models. Cold Reg. Sci. Technol. 97, 132–150.
Gauer, P., 2018. Considerations on scaling behavior in avalanche flow along cycloidal and parabolic tracks. Cold Reg. Sci. Technol. 151, 34–46.
Gauer, P., Issler, D., 2004. Possible erosion mechanisms in snow avalanches. Ann. Glaciol. 38, 384–392.
Gauer, P., Issler, D., Lied, K., Kristensen, K., Iwe, H., Lied, E., Rammer, L., Schreiber, H., 2007. On full-scale avalanche measurements at the Ryggfonn test site. Norway. Cold Reg. Sci. Technol. 49 (1), 39–53.
Gauer, P., Lied, K., Kristensen, K., 2008. On avalanche measurements at the Norwegian full-scale test-site Ryggfonn. Cold Reg. Sci. Technol. 51 (2–3), 138–155.
Gaume, J., van Herwijnen, A., Chambon, G., Wever, N., Schweizer, J., 2017. Snow fracture in relation to slab avalanche release: critical state for the onset of crack propagation. Cryosphere 11 (1), 217–228.
Gaume, J., Gast, T., Teran, J., van Herwijnen, A., Jiang, C., 2018. Dynamic anticrack propagation in snow. Nat. Commun. 9 (1), 3047.
Gaume, J., van Herwijnen, A., Gast, T., Teran, J., Jiang, C., 2019. Investigating the release and flow of snow avalanches at the slope-scale using a unified model based on the material point method. Cold Reg. Sci. Technol. 168, 102847.
Gauthier, D., Jamieson, J.B., 2006. Towards a field test for fracture propagation propensity in weak snowpack layers. J. Glaciol. 52 (176), 164–168.
Gubler, H., 1979. Acoustic emission as an indication of stability decrease in fracture zones of avalanches. J. Glaciol. 22 (86), 186–188.
Hägeli, P., McClung, D.M., 2004. Hierarchy theory as a conceptual framework for scale issues in avalanche forecasting modeling. Ann. Glaciol. 38, 209–214.
Hagenmuller, P., Theile, T.C., Schneebeli, M., 2014. Numerical simulation of microstructural damage and tensile strength of snow. Geophys. Res. Lett. 41 (1), 86–89.
Harbitz, C.B. (Ed.), 1998. EU Programme SAME—A Survey of Computational Models on Snow Avalanche Motion. Norwegian Geotechnical Institute, Oslo, Norway, p. 126. NGI Report 581220.
Heck, M., Hobiger, M., van Herwijnen, A., Schweizer, J., Fäh, D., 2019a. Localization of seismic events produced by avalanches using multiple signal classifications. Geophys. J. Int. 216 (1), 201–217.
Heck, M., van Herwijnen, A., Hammer, C., Hobiger, M., Schweizer, J., Fäh, D., 2019b. Automatic detection of avalanches using combining array classification and localization. Earth Surf. Dyn. 7 (2), 491–503.
Heierli, J., Gumbsch, P., Zaiser, M., 2008. Anticrack nucleation as triggering mechanism for snow slab avalanches. Science 321 (5886), 240–243.
Heilig, A., Mitterer, C., Schmid, L., Wever, N., Schweizer, J., Marshall, H.-P., Eisen, O., 2015. Seasonal and diurnal cycles of liquid water in snow - measurements and modeling. J. Geophys. Res. Earth Surf. 120, 2139–2154.
Helbig, N., van Herwijnen, A., Jonas, T., 2015. Forecasting wet-snow avalanche probability in mountainous terrain. Cold Reg. Sci. Technol. 120, 219–226.
Hendrikx, J., Owens, I., Carran, W., Carran, A., 2005. Avalanche activity in an extreme maritime climate: the application of classification trees for forecasting. Cold Reg. Sci. Technol. 43 (1–2), 104–116.
Höller, P., 2001. Snow gliding and avalanches in a south-facing larch stand. In: Dolman, A.J., Hall, A.J., Kavvas, M.L., Oki, T., Pomeroy, J.W. (Eds.), Soil-Vegetation-Atmosphere Transfer Schemes and Large-Scale Hydrological Models. International Association of Hydrological Sciences, Wallingford, Oxfordshire, U.K, pp. 355–358. IAHS Publ. 270.
Höller, P., 2014. Snow gliding and glide avalanches: a review. Nat. Hazards 71 (3), 1259–1288.
in der Gand, H.R., Zupančič, M., 1966. Snow gliding and avalanches. In: Symposium at Davos 1965- Scientific Aspects of Snow and Ice Avalanches, IAHS Publication. vol. 69. International Association of Hydrological Sciences, Wallingford, Oxfordshire, U.K., Wallingford, U.K, pp. 230–242.
IPCC, 2019. IPCC Special Report on the Ocean and Cryosphere in a Changing Climate [H.-O. Pörtner, D.C. Roberts, V. Masson-Delmotte, P. Zhai, M. Tignor, E. Poloczanska, K. Mintenbeck, A. Alegría, M. Nicolai, A. Okem, J. Petzold, B. Rama, N.M. Weyer (eds.)]. In press.

Jamieson, J.B., 1995. Avalanche Prediction for Persistent Snow Slabs. Ph.D. Thesis, University of Calgary, Calgary AB, Canada. 258 pp.
Jamieson, B., 2001. Snow avalanches. In: Brooks, G.R. (Ed.), A Synthesis of Geological Hazards in Canada. Bulletin 548. Geological Survey of Canada, pp. 81–100.
Jamieson, J.B., 2006. Formation of refrozen snowpack layers and their role in slab avalanche release. Rev. Geophys. 44 (2). 2005RG000176.
Jamieson, J.B., Stethem, C.J., Schaerer, P., McClung, D.M., 2002. Land Managers Guide to Snow Avalanche Hazards in Canada. Canadian Avalanche Association, Revelstoke BC, Canada. 28 pp.
Jomelli, V., Bertran, P., 2001. Wet snow avalanche deposits in the French Alps: structure and sedimentology. Geogr. Ann. A 83A (1–2), 15–28.
Kaempfer, T.U., Schneebeli, M., 2007. Observation of isothermal metamorphism of new snow and interpretation as a sintering process. J. Geophys. Res. 112 (D24), D24101.
Kattelmann, R., 1985. Wet slab instability. In: Proceedings International Snow Science Workshop, Aspen, Colorado, U.S.A., 24-27 October 1984. ISSW 1984 Workshop Committee, Aspen CO, U.S.A, pp. 102–108.
Kern, M., Bartelt, P., Sovilla, B., Buser, O., 2009. Measured shear rates in large dry and wet snow avalanches. J. Glaciol. 55 (190), 327–338.
Kirchner, H.O.K., Michot, G., Suzuki, T., 2000. Fracture toughness of snow in tension. Phil. Mag. A 80 (5), 1265–1272.
Köhler, A., Fischer, J.T., Scandroglio, R., Bavay, M., McElwaine, J., Sovilla, B., 2018. Cold-to-warm flow regime transition in snow avalanches. Cryosphere 12 (12), 3759–3774.
LaChapelle, E.R., 1980. The fundamental process in conventional avalanche forecasting. J. Glaciol. 26 (94), 75–84.
Lackinger, B., 1987. Stability and fracture of the snow pack for glide avalanches. In: Salm, B., Gubler, H. (Eds.), Symposium at Davos 1986- Avalanche Formation, Movement and Effects, IAHS Publ., 162. International Association of Hydrological Sciences, Wallingford, Oxfordshire, U.K, pp. 229–241.
Lehning, M., Bartelt, P., Brown, R.L., Russi, T., Stöckli, U., Zimmerli, M., 1999. Snowpack model calculations for avalanche warning based upon a new network of weather and snow stations. Cold Reg. Sci. Technol. 30 (1–3), 145–157.
Lehning, M., Bartelt, P., Brown, R.L., Fierz, C., 2002a. A physical SNOWPACK model for the Swiss avalanche warning; Part III: meteorological forcing, thin layer formation and evaluation. Cold Reg. Sci. Technol. 35 (3), 169–184.
Lehning, M., Bartelt, P., Brown, R.L., Fierz, C., Satyawali, P.K., 2002b. A physical SNOWPACK model for the Swiss avalanche warning; Part II. Snow microstructure. Cold Reg. Sci. Technol. 35 (3), 147–167.
Lehning, M., Völksch, I., Gustafsson, D., Nguyen, T.A., Stähli, M., Zappa, M., 2006. ALPINE3D: a detailed model of mountain surface processes and its application to snow hydrology. Hydrol. Process. 20 (10), 2111–2128.
Leitinger, G., Höller, P., Tasser, E., Walde, J., Tappeiner, U., 2008. Development and validation of a spatial snowglide model. Ecol. Model. 211 (3–4), 363–374.
Lied, K., Bakkehoi, S., 1980. Empirical calculations of snow-avalanche run-out distance based on topographic parameters. J. Glaciol. 26 (94), 165–177.
Matzl, M., Schneebeli, M., 2006. Measuring specific surface area of snow by near infrared photography. J. Glaciol. 42 (179), 558–564.
Mayer, S., van Herwijnen, A., Ulivieri, G., Schweizer, J., 2020. Evaluating the performance of an operational infrasound avalanche detection system at three locations in the Swiss Alps during two winter seasons. Cold Reg. Sci. Technol. 173, 102962.
McCammon, I., Hägeli, P., 2007. An evaluation of rule-based decision tools for travel in avalanche terrain. Cold Reg. Sci. Technol. 47 (1–2), 193–206.
McClung, D.M., 1979. Shear fracture precipitated by strain softening as a mechanism of dry slab avalanche release. J. Geophys. Res. 84 (87), 3519–3526.

McClung, D.M., 1981a. Fracture mechanical models of dry slab avalanche release. J. Geophys. Res. 86 (B11), 10783–10790.
McClung, D.M., 1981b. A physical theory of snow gliding. Can. Geotech. J. 18 (1), 86–94.
McClung, D.M., Clarke, G.K.C., 1987. The effects of free water on snow gliding. J. Geophys. Res. 92 (B7), 6301–6309.
McClung, D.M., Mears, A.I., 1991. Extreme value prediction of snow avalanche runout. Cold Reg. Sci. Technol. 19, 163–175.
McClung, D.M., Schaerer, P.A., 1985. Characteristics of flowing snow and avalanche impact pressures. Ann. Glaciol. 6, 9–14.
McClung, D.M., Schaerer, P., 2006. The Avalanche Handbook. The Mountaineers Books, Seattle WA, U.S.A. 342 pp.
McClung, D.M., Schweizer, J., 1999. Skier triggering, snow temperatures and the stability index for dry slab avalanche initiation. J. Glaciol. 45 (150), 190–200.
McClung, D.M., Tweedy, J., 1994. Numerical avalanche prediction. Kootenay Pass, British Columbia, Canada. J. Glaciol. 40 (135), 350–358.
McClung, D.M., Stethem, C.J., Schaerer, P., Jamieson, J.B., 2002. Guidelines for Snow Avalanche Risk Determination and Mapping in Canada. Canadian Avalanche Association, Revelstoke, BC, Canada. 24 pp.
Mede, T., Chambon, G., Hagenmuller, P., Nicot, F., 2018. Snow failure modes under mixed loading. Geophys. Res. Lett. 45 (24), 13351–13358.
Meister, R., 1995. Country-wide avalanche warning in Switzerland. In: Proceedings International Snow Science Workshop, Snowbird, Utah, U.S.A., 30 October-3 November 1994. ISSW 1994 Organizing Committee, Snowbird UT, USA, pp. 58–71.
Mitterer, C., Schweizer, J., 2012. Towards a better understanding of glide-snow avalanche formation. In: Proceedings ISSW 2012. International Snow Science Workshop, Anchorage AK, U.S.A., 16–21 September 2012, pp. 610–616.
Mitterer, C., Schweizer, J., 2013. Analysis of the snow-atmosphere energy balance during wet-snow instabilities and implications for avalanche prediction. Cryosphere 7 (1), 205–216.
Mitterer, C., Heilig, A., Schweizer, J., Eisen, O., 2011. Upward-looking ground-penetrating radar for measuring wet-snow properties. Cold Reg. Sci. Technol. 69 (2–3), 129–138.
Monti, F., Schweizer, J., Gaume, J., 2014. Deriving snow stability information from simulated snow cover stratigraphy. In: Haegeli, P. (Ed.), Proceedings ISSW 2014. International Snow Science Workshop, Banff, Alberta, Canada, 29 September–3 October 2014, pp. 465–469.
Newesely, C., Tasser, E., Spadinger, P., Cernusca, A., 2000. Effects of land-use changes on snow gliding processes in alpine ecosystems. Basic Appl. Ecol. 1 (1), 61–67.
Nishimura, K., Maeno, N., Kawada, K., Izumi, K., 1993. Structures of snow cloud in dry-snow avalanches. Ann. Glaciol. 18, 173–178.
Painter, T.H., Molotch, N.P., Cassidy, M., Flanner, M., Steffen, K., 2007. Contact spectroscopy for determination of stratigraphy of snow optical grain size. J. Glaciol. 53 (180), 121–127.
Palmer, A.C., Rice, J.R., 1973. The growth of slip surfaces in the progressive failure of over-consolidated clay. Proc. R. Soc. A-Math. Phys. Eng. Sci. 332 (1591), 527–548.
Peitzsch, E., 2008. Wet slabs: what do we really know about them. Avalanche Rev. 26 (4), 20–21.
Peitzsch, E.H., Hendrikx, J., Fagre, D.B., Reardon, B., 2012. Examining spring wet slab and glide avalanche occurrence along the Going-to-the-Sun Road corridor, Glacier National Park, Montana, USA. Cold Reg. Sci. Technol. 78, 73–81.
Perla, R., 1977. Slab avalanche measurements. Can. Geotech. J. 14 (2), 206–213.
Perla, R.I., 1980. Avalanche release, motion, and impact. In: Colbeck, S.C. (Ed.), Dynamics of Snow and Ice Masses. Academic Press, New York, pp. 397–462.
Perla, R., Cheng, T.T., McClung, D.M., 1980. A two-parameter model of snow-avalanche motion. J. Glaciol. 26 (94), 197–207.

Platzer, K., Bartelt, P., Kern, M., 2007. Measurements of dense snow avalanche basal shear to normal stress ratios (S/N). Geophys. Res. Lett. 34 (7).
Pozdnoukhov, A., Matasci, G., Kanevski, M., Purves, R.S., 2011. Spatio-temporal avalanche forecasting with Support Vector Machines. Nat. Hazards Earth Syst. Sci. 11 (2), 367–382.
Prokop, A., 2008. Assessing the applicability of terrestrial laser scanning for spatial snow depth measurements. Cold Reg. Sci. Technol. 54 (3), 155–163.
Rastello, M., Rastello, F., Bellot, H., Ousset, F., Dufour, F., Meier, L., 2011. Size of snow particles in a powder-snow avalanche. J. Glaciol. 57 (201), 151–156.
Reiweger, I., Schweizer, J., 2010. Failure of a layer of buried surface hoar. Geophys. Res. Lett. 37, L24501.
Reiweger, I., Schweizer, J., 2013a. Measuring acoustic emissions in an avalanche starting zone to monitor snow stability. In: Naaim-Bouvet, F., Durand, Y., Lambert, R. (Eds.), Proceedings ISSW 2013. International Snow Science Workshop, Grenoble, France, 7–11 October 2013. ANENA, IRSTEA, Météo-France, Grenoble, France, pp. 942–944.
Reiweger, I., Schweizer, J., 2013b. Weak layer fracture: facets and depth hoar. Cryosphere 7 (5), 1447–1453.
Reiweger, I., Gaume, J., Schweizer, J., 2015. A new mixed-mode failure criterion for weak snowpack layers. Geophys. Res. Lett. 42 (5), 1427–1432.
Reuter, B., Schweizer, J., 2012. The effect of surface warming on slab stiffness and the fracture behavior of snow. Cold Reg. Sci. Technol. 83–84, 30–36.
Reuter, B., Semmel, C., 2018. Backcountry risk assessment based on terrain and snowpack characteristics. In: Fischer, J.-T., Adams, M., Dobesberger, P., Fromm, R., Gobiet, A., Granig, M., Mitterer, C., Nairz, P., Tollinger, C. (Eds.), Proceedings ISSW 2018. International Snow Science Workshop, Innsbruck, Austria, 7–12 October 2018, pp. 1632–1634.
Reuter, B., Schweizer, J., van Herwijnen, A., 2015. A process-based approach to estimate point snow instability. Cryosphere 9, 837–847.
Reuter, B., Richter, B., Schweizer, J., 2016. Snow instability patterns at the scale of a small basin. J. Geophys. Res.-Earth Surf. 121, 257–282.
Reuter, B., Proksch, M., Löwe, H., van Herwijnen, A., Schweizer, J., 2019. Comparing measurements of snow mechanical properties relevant for slab avalanche release. J. Glaciol. 65 (249), 55–67.
Rice, B., Howlett, D., Decker, R., 1997. Preliminary investigations of glide/creep motion sensors in Alta, Utah. In: Proceedings International Snow Science Workshop, Banff, Alberta, Canada, 6–10 October 1996. Canadian Avalanche Association, Revelstoke BC, Canada, pp. 189–194.
Richter, B., Schweizer, J., Rotach, M.W., van Herwijnen, A., 2019. Validating modeled critical crack length for crack propagation in the snow cover model SNOWPACK. Cryosphere 13 (12), 3353–3366.
Rudolf-Miklau, F., Sauermoser, S., Mears, A.I. (Eds.), 2015. The Technical Avalanche Protection Handbook. Wilhelm Ernst & Sohn, Verlag für Architektur und technische Wissenschaften GmbH & Co. KG, Berlin, Germany. 404 pp.
Salm, B., Burkard, A., Gubler, H., 1990. Berechnung von Fliesslawinen. In: Eine Anleitung für Praktiker mit Beispielen. Mitteilungen des Eidg. Instituts für Schnee- und Lawinenforschung. vol. 47. Swiss Federal Institute for Snow and Avalanche Research SLF, Weissfluhjoch/Davos, Switzerland. 37 pp.
Sampl, P., Zwinger, T., 2004. Avalanche simulation with SAMOS. Ann. Glaciol. 38, 393–398.
Schimmel, A., Hübl, J., Koschuch, R., Reiweger, I., 2017. Automatic detection of avalanches: evaluation of three different approaches. Nat. Hazards 87 (1), 83–102.
Schirmer, M., Lehning, M., Schweizer, J., 2009. Statistical forecasting of regional avalanche danger using simulated snow cover data. J. Glaciol. 55 (193), 761–768.
Schirmer, M., Wirz, V., Clifton, A., Lehning, M., 2011. Persistence in intra-annual snow depth distribution: 1. Measurements and topographic control. Water Resour. Res. 47, W09516.
Schmid, L., Heilig, A., Mitterer, C., Schweizer, J., Maurer, H., Okorn, R., Eisen, O., 2014. Continuous snowpack monitoring using upward-looking ground-penetrating radar technology. J. Glaciol. 60 (221), 509–525.

Schneebeli, M., 2004. Mechanisms in wet snow avalanche release. In: Proceedings ISSMA-2004, International Symposium on Snow Monitoring and Avalanches. Snow and Avalanche Study Establishment, India, Manali, India, 12–16 April 2004, pp. 75–77.
Schneebeli, M., Bebi, P., 2004. Snow and avalanche control. In: Evans, J., Burley, J., Youngquist, J. (Eds.), Encyclopedia of Forest Sciences. Elsevier, Oxford, pp. 397–402.
Schneebeli, M., Johnson, J.B., 1998. A constant-speed penetrometer for high-resolution snow stratigraphy. Ann. Glaciol. 26, 107–111.
Schneebeli, M., Sokratov, S.A., 2004. Tomography of temperature gradient metamorphism of snow and associated changes in heat conductivity. Hydrol. Process. 18 (18), 3655–3665.
Schweizer, J., 2004. Snow avalanches. Water Resources Impact 6 (1), 12–18.
Schweizer, J., Föhn, P.M.B., 1996. Avalanche forecasting—an expert system approach. J. Glaciol. 42 (141), 318–332.
Schweizer, J., Jamieson, J.B., 2001. Snow cover properties for skier triggering of avalanches. Cold Reg. Sci. Technol. 33 (2–3), 207–221.
Schweizer, J., Jamieson, J.B., 2003. Snowpack properties for snow profile analysis. Cold Reg. Sci. Technol. 37 (3), 233–241.
Schweizer, J., Jamieson, J.B., 2007. A threshold sum approach to stability evaluation of manual snow profiles. Cold Reg. Sci. Technol. 47 (1–2), 50–59.
Schweizer, J., Jamieson, B., 2010a. On surface warming and snow instability. In: Proceedings ISSW 2010. International Snow Science Workshop, Lake Tahoe CA, U.S.A., 17–22 October 2010, pp. 619–622.
Schweizer, J., Jamieson, J.B., 2010b. Snowpack tests for assessing snow-slope instability. Ann. Glaciol. 51 (54), 187–194.
Schweizer, J., Lütschg, M., 2001. Characteristics of human-triggered avalanches. Cold Reg. Sci. Technol. 33 (2–3), 147–162.
Schweizer, J., Reuter, B., van Herwijnen, A., Richter, B., Gaume, J., 2016. Temporal evolution of crack propagation propensity in snow in relation to slab and weak layer properties. Cryosphere 10 (6), 2637–2653.
Schweizer, J., van Herwijnen, A., 2013. Can near real-time avalanche occurrence data improve avalanche forecasting? In: Naaim-Bouvet, F., Durand, Y., Lambert, R. (Eds.), Proceedings ISSW 2013. International Snow Science Workshop, Grenoble, France, 7–11 October 2013. ANENA, IRSTEA, Météo-France, Grenoble, France, pp. 195–198.
Schweizer, J., Jamieson, J.B., Skjonsberg, D., 1998. Avalanche forecasting for transportation corridor and backcountry in Glacier National Park (BC, Canada). In: Hestnes, E. (Ed.), 25 Years of Snow Avalanche Research, Voss, Norway, 12–16 May 1998. NGI Publication. Norwegian Geotechnical Institute, Oslo, Norway, pp. 238–243.
Schweizer, J., Jamieson, J.B., Schneebeli, M., 2003. Snow avalanche formation. Rev. Geophys. 41 (4), 1016.
Schweizer, J., Michot, G., Kirchner, H.O.K., 2004. On the fracture toughness of snow. Ann. Glaciol. 38, 1–8.
Schweizer, J., Bellaire, S., Fierz, C., Lehning, M., Pielmeier, C., 2006. Evaluating and improving the stability predictions of the snow cover model SNOWPACK. Cold Reg. Sci. Technol. 46 (1), 52–59.
Schweizer, J., Mitterer, C., Stoffel, L., 2009. On forecasting large and infrequent snow avalanches. Cold Reg. Sci. Technol. 59 (2–3), 234–241.
Schweizer, J., van Herwijnen, A., Reuter, B., 2011. Measurements of weak layer fracture energy. Cold Reg. Sci. Technol. 69 (2–3), 139–144.
Schweizer, J., Reuter, B., van Herwijnen, A., Gaume, J., 2016. Avalanche release 101. In: Greene (Ed.), Proceedings ISSW 2016. International Snow Science Workshop, Breckenridge CO, U.S.A., 3–7 October 2016, pp. 1–11.
Schweizer, J., Mitterer, C., Techel, F., Stoffel, A., Reuter, B., 2020. On the relation between avalanche occurrence and avalanche danger level. Cryosphere 14 (2), 737–750.
Sigrist, C., Schweizer, J., 2007. Critical energy release rates of weak snowpack layers determined in field experiments. Geophys. Res. Lett. 34 (3), L03502.

Simenhois, R., Birkeland, K., 2010. Meteorological and environmental observations from three glide avalanche cycles and the resulting hazard management technique. In: Proceedings ISSW 2010. International Snow Science Workshop, Lake Tahoe CA, U.S.A., 17–22 October 2010, pp. 846–853.
Simioni, S., Sidler, R., Dual, J., Schweizer, J., 2015. Field measurements of snowpack response to explosive loading. Cold Reg. Sci. Technol. 120, 179–190.
Simioni, S., Dual, J., Schweizer, J., 2017. Snowpack response to directed gas explosions on level ground. Cold Reg. Sci. Technol. 144, 73–88.
Sommerfeld, R.A., 1977. Preliminary observations of acoustic emissions preceding avalanches. J. Glaciol. 19 (81), 399–409.
Sovilla, B., 2004. Field Experiments and Numerical Modelling of Mass Entrainment and Deposition Processes in Snow Avalanches. Ph.D. Thesis, ETH Zurich, Zurich, Switzerland. 190 pp.
Sovilla, B., Schaer, M., Kern, M., Bartelt, P., 2008. Impact pressures and flow regimes in dense snow avalanches observed at the Vallée de la Sionne test site. J. Geophys. Res. Earth Surf. 113 (F1), F01010.
Sovilla, B., McElwaine, J.N., Schaer, M., Vallet, J., 2010. Variation of deposition depth with slope angle in snow avalanches: measurements from Vallée de la Sionne. J. Geophys. Res. Earth Surf. 115 (F2), F02016.
St. Lawrence, W.F., Bradley, C.C., 1977. Spontaneous fracture initiation in mountain snow-packs. J. Glaciol. 19 (81), 411–417.
Statham, G., Haegeli, P., Greene, E., Birkeland, K., Israelson, C., Tremper, B., Stethem, C., McMahon, B., White, B., Kelly, J., 2018. A conceptual model of avalanche hazard. Nat. Hazards 90 (2), 663–691.
Steinkogler, W., Gaume, J., Löwe, H., Sovilla, B., Lehning, M., 2015. Granulation of snow: from tumbler experiments to discrete element simulations. J. Geophys. Res. Earth Surf. 120 (6), 1107–1126.
Stimberis, J., Rubin, C., 2005. Glide avalanche detection on a smooth rock slope, Snoqualmie Pass, Washington. In: Elder, K. (Ed.), Proceedings ISSW 2004. International Snow Science Workshop, Jackson Hole WY, U.S.A., 19–24 September 2004, pp. 608–610.
Stimberis, J., Rubin, C.M., 2011. Glide avalanche response to an extreme rain-on-snow event, Snoqualmie Pass, Washington, USA. J. Glaciol. 57 (203), 468–474.
Techel, F., Pielmeier, C., 2009. Wet snow diurnal evolution and stability assessment. In: Schweizer, J., van Herwijnen, A. (Eds.), International Snow Science Workshop ISSW, Davos, Switzerland, 27 September–2 October 2009. Swiss Federal Institute for Forest, Snow and Landscape Research WSL, pp. 256–261.
Swift, D.A., Cook, S., Heckmann, T., Gärtner-Roer, I., Korup, O., Moore, J., 2021. Ice and snow as land-forming agents. In: Haeberli, W., Whiteman, C. (Eds.), Snow and Ice-Related Hazards, Risks and Disasters. Elsevier, pp. 165–198.
Techel, F., Müller, K., Schweizer, J., 2020. On the importance of snowpack stability, its frequency distribution, and avalanche size in assessing the avalanche danger level: a data-driven approach. Cryosphere, 1–36. In press.
Teich, M., Marty, C., Gollut, C., Grêt-Regamey, A., Bebi, P., 2012. Snow and weather conditions associated with avalanche releases in forests: rare situations with decreasing trends during the last 41 years. Cold Reg. Sci. Technol. 83–84, 77–88.
Teich, M., Giunta, A.D., Hagenmuller, P., Bebi, P., Schneebeli, M., Jenkins, M.J., 2019. Effects of bark beetle attacks on forest snowpack and avalanche formation—implications for protection forest management. For. Ecol. Manage. 438, 186–203.
Trautman, S., 2008. Investigations into wet snow. Avalanche Rev. 26 (4), 16–17. 21.
UNESCO, 1981. Avalanche Atlas-Illustrated International Avalanche Classification. International Commission for Snow and Ice of the International Association of Hydrological Sciences. UNESCO, Paris, France. 265 pp.
van Herwijnen, A., Heierli, J., 2009. Measurements of weak snowpack layer friction. In: Schweizer, J., van Herwijnen, A. (Eds.), International Snow Science Workshop ISSW, Davos, Switzerland, 27 September–2 October 2009. Swiss Federal Institute for Forest, Snow and Landscape Research WSL, pp. 112–114.
van Herwijnen, A., Jamieson, B., 2005. High-speed photography of fractures in weak snowpack layers. Cold Reg. Sci. Technol. 43 (1–2), 71–82.

van Herwijnen, A., Jamieson, J.B., 2007. Fracture character in compression tests. Cold Reg. Sci. Technol. 47 (1–2), 60–68.
van Herwijnen, A., Schweizer, J., 2011a. Monitoring avalanche activity using a seismic sensor. Cold Reg. Sci. Technol. 69 (2–3), 165–176.
van Herwijnen, A., Schweizer, J., 2011b. Seismic sensor array for monitoring an avalanche start zone: design, deployment and preliminary results. J. Glaciol. 57 (202), 267–276.
van Herwijnen, A., Simenhois, R., 2012. Monitoring glide avalanches using time-lapse photography. In: Proceedings ISSW 2012. International Snow Science Workshop, Anchorage AK, U.S.A., 16-21 September 2012, pp. 899–903.
van Herwijnen, A., Bellaire, S., Schweizer, J., 2009. Comparison of micro-structural snowpack parameters derived from penetration resistance measurements with fracture character observations from compression tests. Cold Reg. Sci. Technol. 59 (2–3), 193–201.
van Herwijnen, A., Schweizer, J., Heierli, J., 2010. Measurement of the deformation field associated with fracture propagation in weak snowpack layers. J. Geophys. Res. 115, F03042.
van Herwijnen, A., Berthod, N., Simenhois, R., Mitterer, C., 2013. Using time-lapse photography in avalanche research. In: Naaim-Bouvet, F., Durand, Y., Lambert, R. (Eds.), Proceedings ISSW 2013. International Snow Science Workshop, Grenoble, France, 7–11 October 2013. ANENA, IRSTEA, Météo-France, Grenoble, France, pp. 950–954.
van Herwijnen, A., Gaume, J., Bair, E.H., Reuter, B., Birkeland, K.W., Schweizer, J., 2016. Estimating the effective elastic modulus and specific fracture energy of snowpack layers from field experiments. J. Glaciol. 62 (236), 997–1007.
Vera Valero, C., Wikstroem, J.K., Bühler, Y., Bartelt, P., 2015. Release temperature, snow cover entrainment and the thermal flow regime of snow avalanches. J. Glaciol. 61 (225), 173–184.
Vernay, M., Lafaysse, M., Mérindol, L., Giraud, G., Morin, S., 2015. Ensemble forecasting of snowpack conditions and avalanche hazard. Cold Reg. Sci. Technol. 120, 251–262.
Vionnet, V., Brun, E., Morin, S., Boone, A., Faroux, S., Le Moigne, P., Martin, E., Willemet, J.M., 2012. The detailed snowpack scheme Crocus and its implementation in SURFEX v7.2. Geosci. Model Dev. 5 (3), 773–791.
Walters, D.J., Adams, E.E., 2014. Quantifying anisotropy from experimental testing of radiation recrystallized snow layers. Cold Reg. Sci. Technol. 97, 72–80.
Wautier, A., Geindreau, C., Flin, F., 2015. Linking snow microstructure to its macroscopic elastic stiffness tensor: a numerical homogenization method and its application to 3-D images from X-ray tomography. Geophys. Res. Lett. 42 (19). 2015GL065227.
Wever, N., Vera Valero, C., Fierz, C., 2016. Assessing wet snow avalanche activity using detailed physics based snowpack simulations. Geophys. Res. Lett. 43, 5732–5740.
Wilhelm, C., Wiesinger, T., Bründl, M., Ammann, W.J., 2001. The avalanche winter 1999 in Switzerland - an overview. In: Proceedings International Snow Science Workshop, Big Sky, Montana, U.S.A., 1-6 October 2000. Montana State University, Bozeman MT, USA, pp. 487–494.
Wilson, A., Statham, G., Bilak, R., Allen, B., 1997. Glide avalanche forecasting. In: Proceedings International Snow Science Workshop, Banff, Alberta, Canada, 6-10 October 1996. Canadian Avalanche Association, Revelstoke BC, Canada, pp. 200–202.
Yamanoi, K., Endo, Y., 2002. Dependence of shear strength of snow cover on density and water content (in Japanese with English Abstract). Seppyo, J. Jpn. Soc. Snow Ice 64 (4), 443–451.